Supporting Information

Isoreticular 3D Covalent Organic Frameworks with non-interpenetrated pcu-derived dia Topology: Pore Regulation from Micropores to Mesopores

Xilin Li[a], Tongyi Zhao[a], Fengzhen Wang[a], Wenxuan Wu[a], Yali Sun[a], Hao Ren[a], Fuxing Sun[*a]

[a] *State Key Laboratory of Inorganic Synthesis and Preparative Chemistry, Jilin University, Changchun, 130012, P. R. China.*
E-mail: fxsun@jlu.edu.cn; *Fax*: +86-431-85168331; *Tel*: +86-431-85168331

Table of Contents

Section S1. The dia topology COFs

Table S1. The **dia** topology COFs in literature.

Monomer 1	Monomer 2	Materials	int.deg.[a]	Ref.
4-c node and 2-c linker				
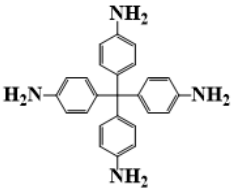	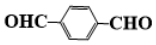	COF-300	5	[S1]
	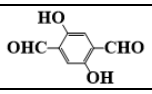	COF-300-B	5	[S2]
	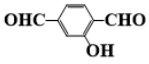	COF-300-E	5	
	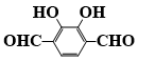	COF-300-G	5	
	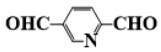	COF-300-H	5	
	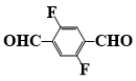	COF-300-I	5	
	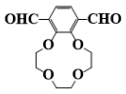	JUC-591	7	[S3]
		PI-COF-5	4	[S4]
	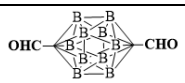	TAPM-DFCB-COF	7	[S5]
	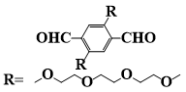	TK-COF-1	1	[S6]
		TK-COF-3	2	
	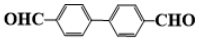	COF-320	9	[S7]
	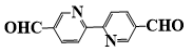	LZU-301	9	[S8]
	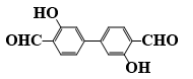	TAPM-DHBD	9	[S9]
	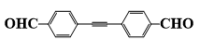	CPOF-2	9	[S10]
		CPOF-3	11	
	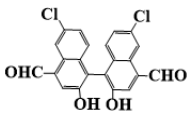	CCOF 15	9	[S11]
	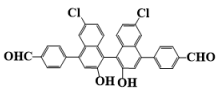	CCOF 16	11	

	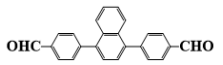	JUC-575	10	[S12]
		JUC-576	10	
	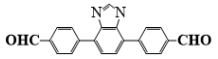	LZU-79	10	[S13]
	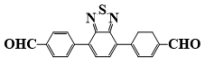	JUC-636	10	[S14]
	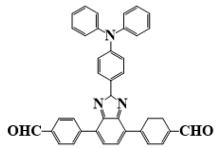	JUC-635	10	
	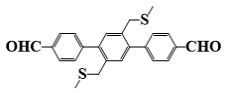	JUC-571	10	[S15]
	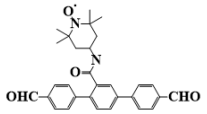	JUC-565	10	[S16]
	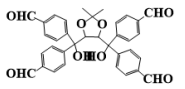	CCOF-5	4	[S17]
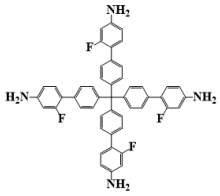	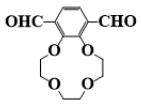	JUC-590	5	[S3]
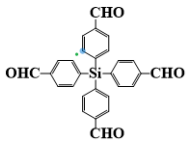	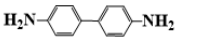	LZU-310	9	[S18]
	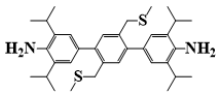	JUC-570	10	[S15]
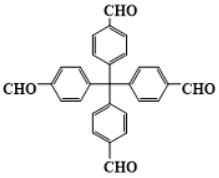	N_2H_4	3D-HNU-5	2	[S19]
	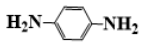	COF-303	7	[S13]
	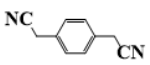	TFPM-PDAN	5	[S20]
		TFPM-PZI	5	[S21]
	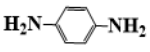	3D-IL-COF-1	5	[S22]
	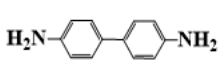	3D-IL-COF-2	9	
	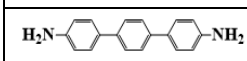	3D-IL-COF-3	11	

	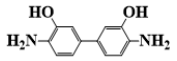	3D-OH-COF	9	[S23]
	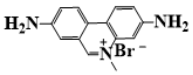	3D-ionic-COF-1	3	[S24]
	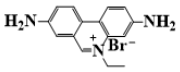	3D-ionic-COF-2	3	
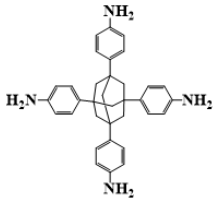	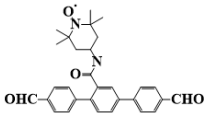	JUC-566	10	[S16]
	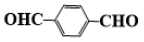	COF-DL-229	8	[S25]
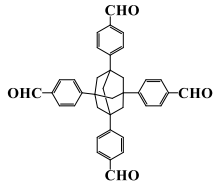	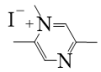	TAPM-PZI	8	[S21]
	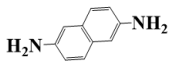	JLNU-320	2	[S26]
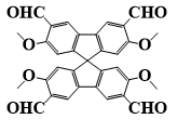	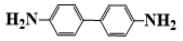	JUC-550	1	[S27]
	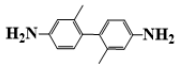	JUC-551	1	
	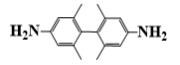	JUC-552	1	
	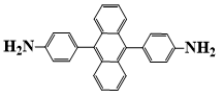	NKCOF-14	4	[S28]
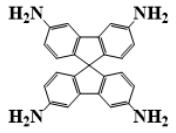	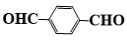	SP-3D-COF 1	6	[S29]
	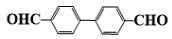	SP-3D-COF 2	7	
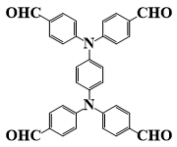	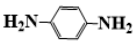	3D-PATB-COF	12	[S30]
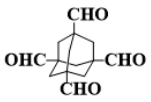	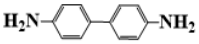	LZU-311	6	[S18]
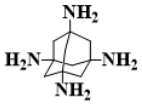		PI-COF-4	1	[S4]
	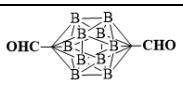	TAA-DFCB-COF	7	[S5]
4-c node and 4-c node				

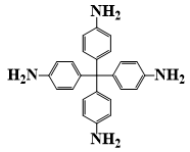	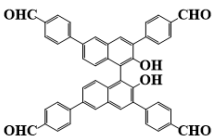	CCOF-22-OH	5	[S31]
	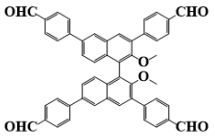	CCOF-22-OMe	4	
	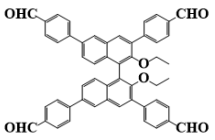	CCOF-22-OEt	4	
	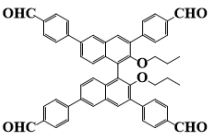	CCOF-22-O^{n}Pr	1	
	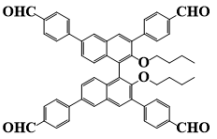	CCOF-22-O^{n}Bu	1	
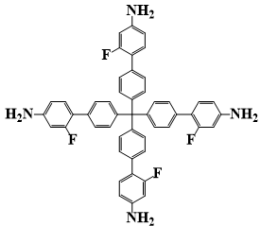	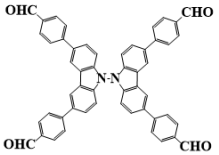	JUC-620	7	[S32]
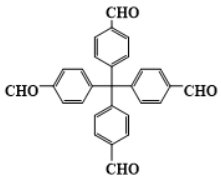	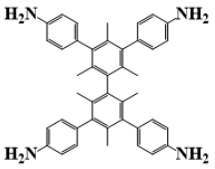	BMTA-TFPM-COF	1	[S33]
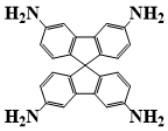	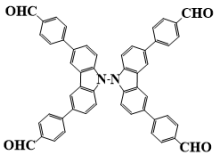	SP-CA-COF-IM	4	[S34]
6-c node and 2-c linker				
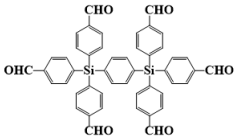	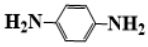	JUC-300	1	This work
	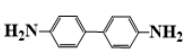	JUC-301	1	This work
	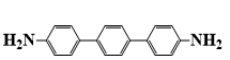	JUC-302	1	This work

[a] Interpenetrating degree.

Section S2. Materials and Instruments

All reagents and solvents used in this work, unless otherwise noted, were purchased from Energy Chemical Co. and used without further purification. All gases for sorption analysis were supplied at a purity of ≥99.9%. Reactions were carried out under Ar atmosphere using standard Schlenk techniques.

NMR spectra were recorded on a Bruker 300 NMR spectrometer at 300 MHz (^{1}H) and referenced against the residual ^{1}H signal of the solvent. The Elemental analysis (for C, H, N) was carried out using a Perkin Elmer 2400 Series. Fourier transform infrared (FTIR) spectra were recorded using a Bruker VERTEX 80v FTIR Spectrometer. The solid-state ^{13}C NMR was performed by using a Bruker Avance 600 MHz Solid-State NMR Spectrometer. Thermogravimetric analysis (TGA) was performed using a Netzch Sta 449c thermal analyzer system at the heating rate of 10 °C/min from room temperature to 800 °C in an air atmosphere. Powder X-ray diffraction (PXRD) data were collected using a Bruker AXS D8 Advance diffractometer with Cu Kα-radiation (λ = 1.5418 Å) over the range of 2θ = 3−40.0° with a step size of 0.02° and 2 s per step. Scanning Electron Microscopy (SEM) was carried out using a JEOL JEM 6700. Samples were prepared by depositing the dry powders on a silicon disk. Transmission electron microscopy (TEM) image was obtained on JEM-2100 transmission electron microscopy. The nitrogen adsorption isotherms were measured on a Quanta Autosorb-1c analyzer at 77 K.

The incorporation of a protein, myoglobin (Mb), in COFs was monitored through UV-Vis spectrophotometry. Typically, 150 μg mL^{-1} of Mb was prepared in 10.0 mL phosphate buffer solution (PBS, pH = 7.4). And then, 4.0 mg freshly activated COF powder was added into the solution and the solution was placed in an incubator at 25 °C. The supernatant was scanned at different time points to determine uptake of Mb by the decrease of the Soret band at 409 nm. The adsorption capacity at different time points Q_t (mg g^{-1}) was calculated with equation, $Q_t = \frac{(C_0 - C_t)V}{m}$, where m (mg) is the mass of the adsorbent; V (mL) is the volume of solution; C_0 and C_t (μg mL^{-1}) are the concentrations of the protein at initial and specific time point, respectively.

Section S3. Synthetic procedures

Scheme S1. Synthesis of the monomer for COFs.

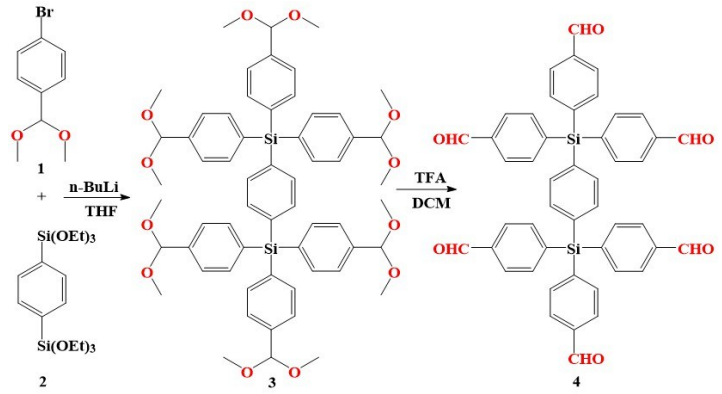

Synthesis of 1,4-bis(tris(4-(dimethoxymethyl)phenyl)silyl)benzene (3) : 4-Bromobenzaldehyde dimethyl acetal (3.7 g, 16.0 mmol) was dissolved in dry THF (30 mL) under nitrogen. *n*-Butyllithium (*n*-BuLi) solution in hexane (1.6 M, 10 mL, 16 mmol) was added slowly at -78 ℃. The resultant reaction mixture was allowed to stir for two h at -78 °C before warming to 0 °C. 1, 4-Bis(trisethoxysilyl)benzene (1 ml, 2.52 mmol) was then added dropwise, and the reaction mixture stirred for 12 hours. The reaction mixture was quenched with 10 mL of distilled water and extracted with ethyl acetate (3 × 50 mL). The ethyl acetate solution was washed with brine, and dried over Na_2SO_4. After that, the solvent was evaporated under reduced pressure and the crude product was purified by column chromatography to yield compound **3** as a yellow solid (1.4 g, 60% yield) .^{1}H NMR (300 MHz, $CDCl_3$, ppm): δ = 7.55 (m, 16H), 7.44(d, 12H), 5.39 (s, 6H), 3.34(s, 36H), ^{13}C NMR (75 MHz, $CDCl_3$, ppm): δ = 136.29, 126.13, 103.20, 52.90.

Synthesis of 1,4-phenylenebis(tris(4-formylphenyl)silane) (PBTSi-6CHO, 4): Trifluoroacetic acid (10 mL) was added dropwise into a solution of compound 3 (1.4 g, 3.1 mmol) in CH_2Cl_2 (30 mL), and the mixture was stirred overnight at room temperature. Subsequently, the reaction was quenched by adding saturated sodium carbonate solution to pH = 10. The mixture was extracted with ethyl acetate (3 × 50 mL) and washed with brine, and dried over anhydrous Na_2SO_4 . After that, the solvent was removed under vacuum to give **4** as a white solid (0.8g, 60% yield). ^{1}H NMR

(300 MHz, $CDCl_3$, ppm): δ = 10.08 (s, 6H), 7.92 (d, J = 7.8 Hz,12H), 7.73 (d, J = 7.8 Hz,12H),7.61 (s, 4H). ^{13}C NMR (100 MHz, $CDCl_3$, ppm): δ = 192.0, 140.0, 137.5, 136.7, 135.9, 129.0.

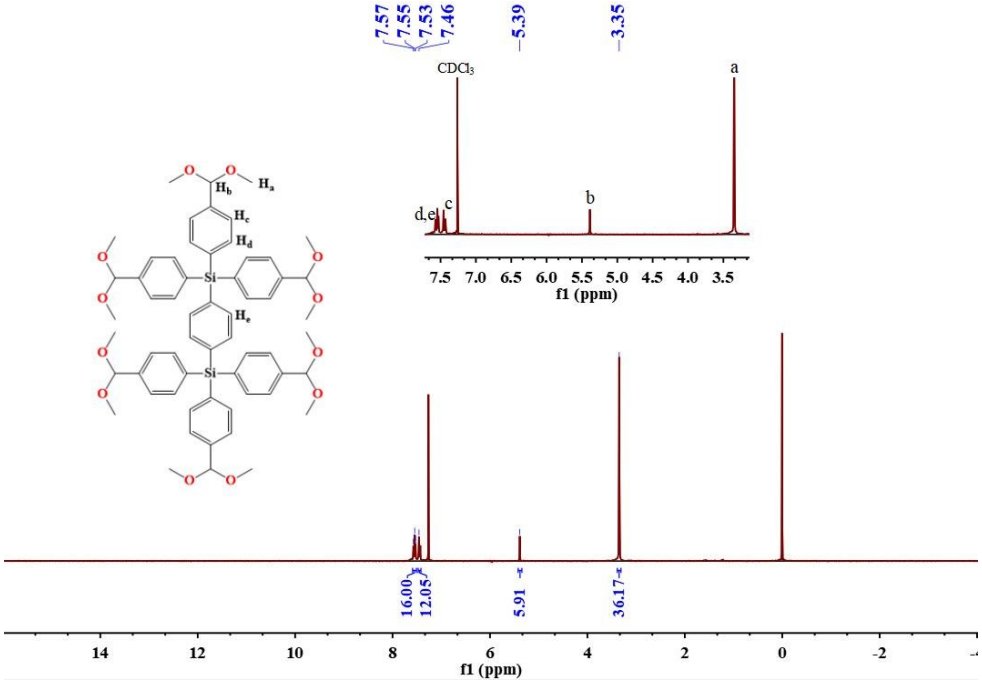

Figure S1. 1H NMR spectra of **3**.

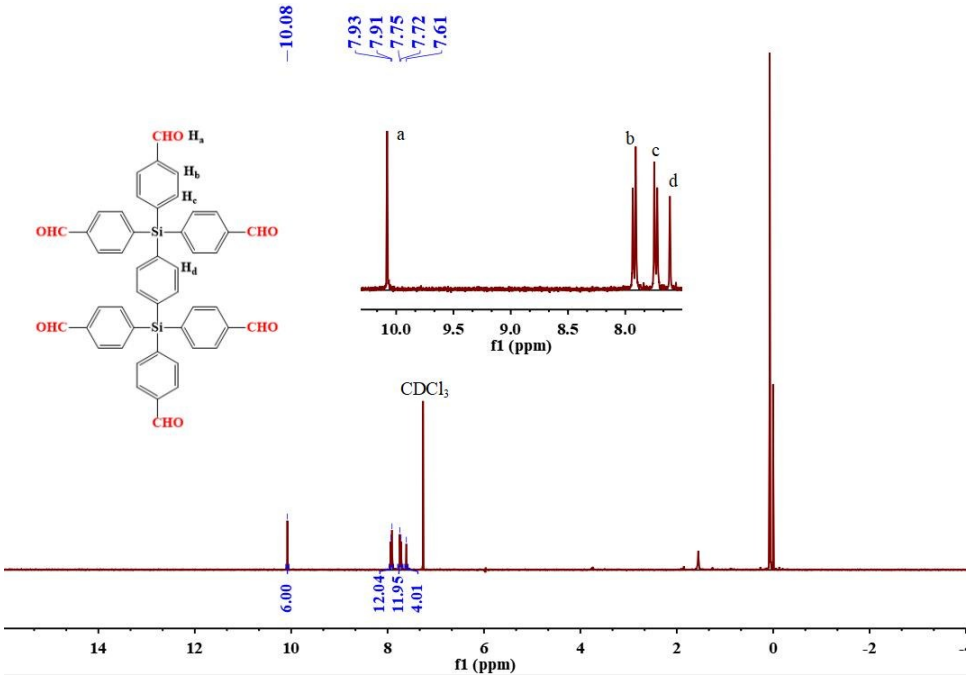

Figure S2. ^1H NMR spectra of **4**.

Scheme S2. Synthesis of JUC-300.

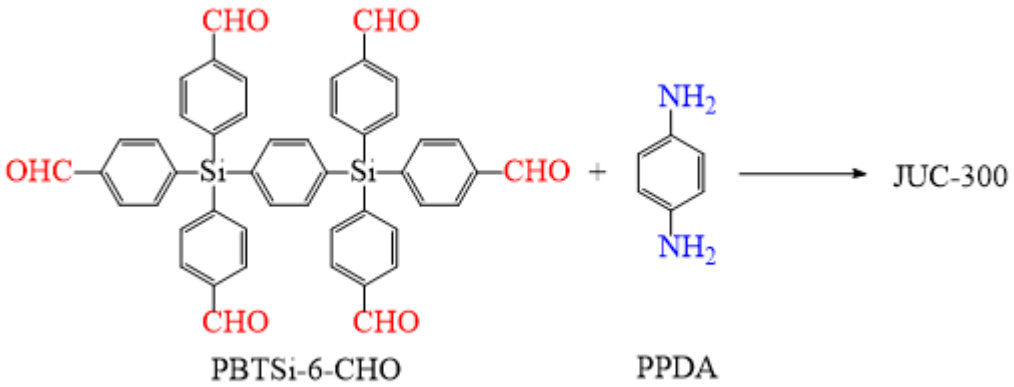

Synthesis of JUC-300: A Pyrex tube was charged with PBTSi-6-CHO (20 mg, 0.04mmol), PPDA(10 mg, 0.12 mmol), THF (1.0 mL), Mesitylene (1.0 mL) and 6 M aqueous acetic acid (0.2 mL). The solution was sonicated for 30 minutes, The Pyrex tube was flash frozen in a liquid nitrogen bath, After being degassed by freeze-pump-thaw technique for three times and then sealed under vacuum, warming to room temperature. The reaction was heated to 120 ℃ for 3 days, As a result, a brown powder was isolated by centrifugation and washed with THF (3 × 5.0 mL), then activated under dynamic vacuum at 120 °C for 12 h to yield the crystalline powder in 90% yield.

Elem. Anal. of JUC-300: Calcd. for $C_{66}H_{46}N_6Si_2$: C, 80.90%; H, 4.70%; N, 8.58%. Found: C, 74.30; H, 5.02%; N, 7.48%.

Scheme S3. Synthesis of JUC-301.

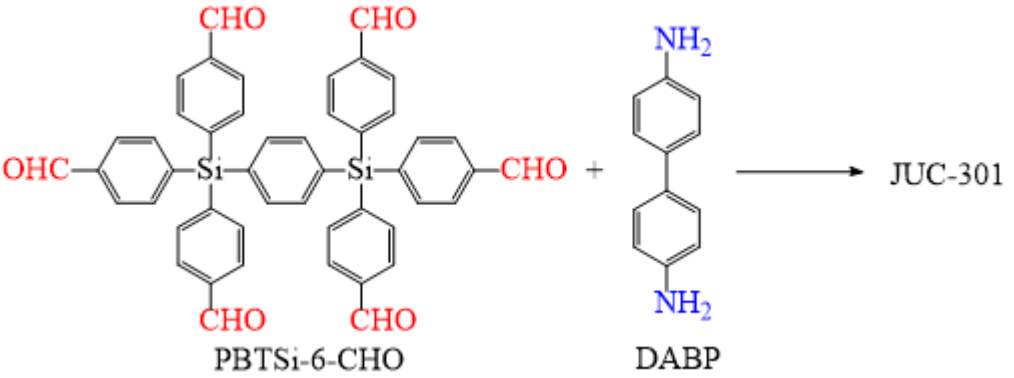

Synthesis of JUC-301: A Pyrex tube was charged with PBTSi-6-CHO (20 mg, 0.04mmol), DABP (15 mg, 0.12 mmol), THF (1.0 mL), Mesitylene (1.0 mL) and 6 M aqueous acetic acid (0.2 mL). The solution was sonicated for 30 minutes, The Pyrex

tube was flash frozen in a liquid nitrogen bath, After being degassed by freeze-pump-thaw technique for three times and then sealed under vacuum, warming to room temperature. The reaction was heated to 120 ℃ for 3 days, As a result, a brown powder was isolated by centrifugation and washed with THF (3 × 5.0 mL), yield the crystalline powder in 87% yield.

Elem. Anal. of JUC-301: Calcd. for $C_{84}H_{58}N_6Si_2$: C, 83.58%; H, 4.81%; N, 6.96%. Found: C, 81.71%; H, 5.55%; N, 5.56%.

Scheme S4. Synthesis of JUC-302**.**

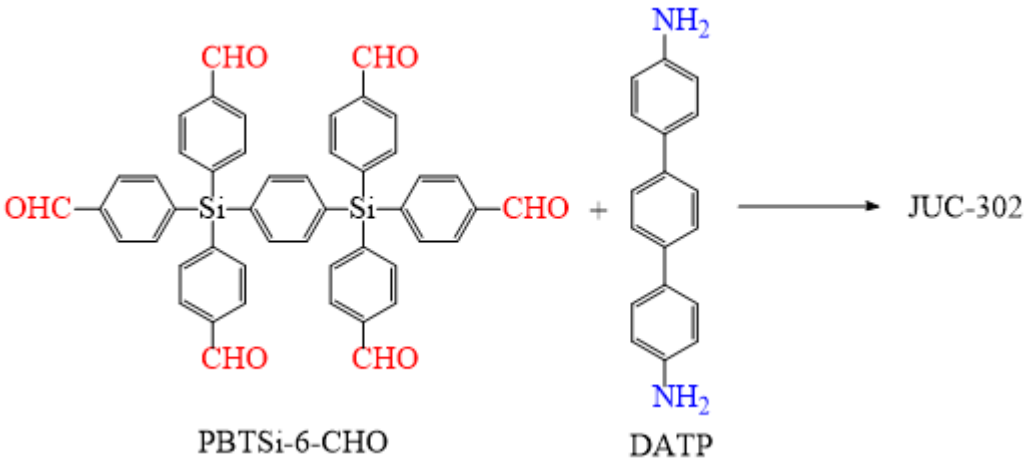

Synthesis of JUC-302: A Pyrex tube was charged with PBTSi-6-CHO (20 mg, 0.04mmol), DATP (20 mg, 0.12 mmol), THF (1.0 mL), Mesitylene (1.0 mL) and 6 M aqueous acetic acid (0.2 mL). The solution was sonicated for 30 minutes, The Pyrex tube was flash frozen in a liquid nitrogen bath, After being degassed by freeze-pump-thaw technique for three times and then sealed under vacuum, warming to room temperature. The reaction was heated to 120 ℃ for 3 days, As a result, a brown powder was isolated by centrifugation and washed with THF (3 × 5.0 mL), yield the crystalline compound in 80% yield.

Elem. Anal. of JUC-302: Calcd. for $C_{84}H_{58}N_6Si_2$: C, 85.4%; H, 4.88%; N, 5.86%. Found: C, 82.77%; H, 6.075%; N, 4.39%.

Section S4. FT-IR and NMR spectra

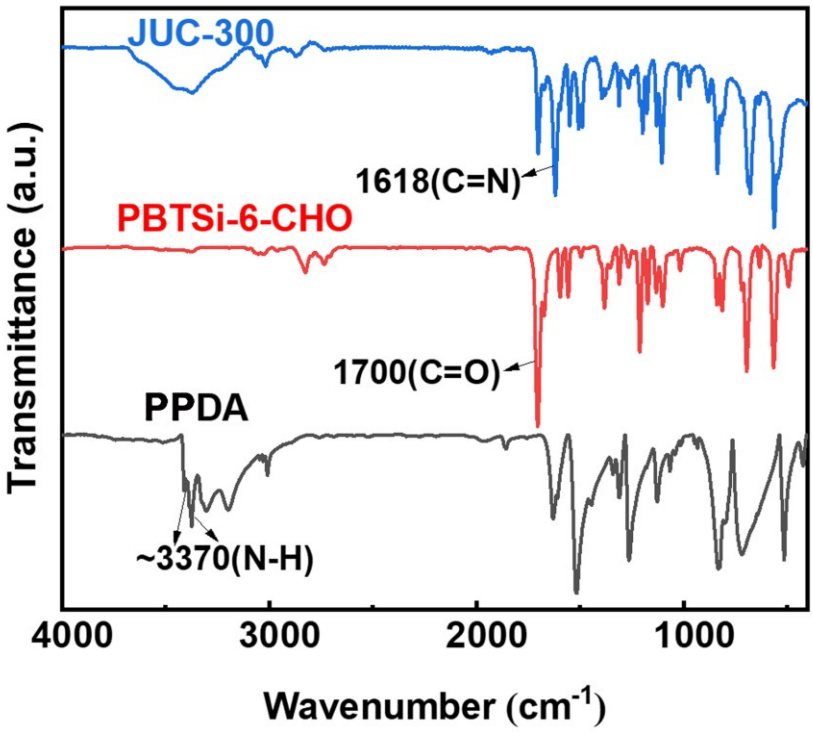

Figure S3. FT-IR spectra of PPDA, PBTSi-6-CHO and JUC-300.

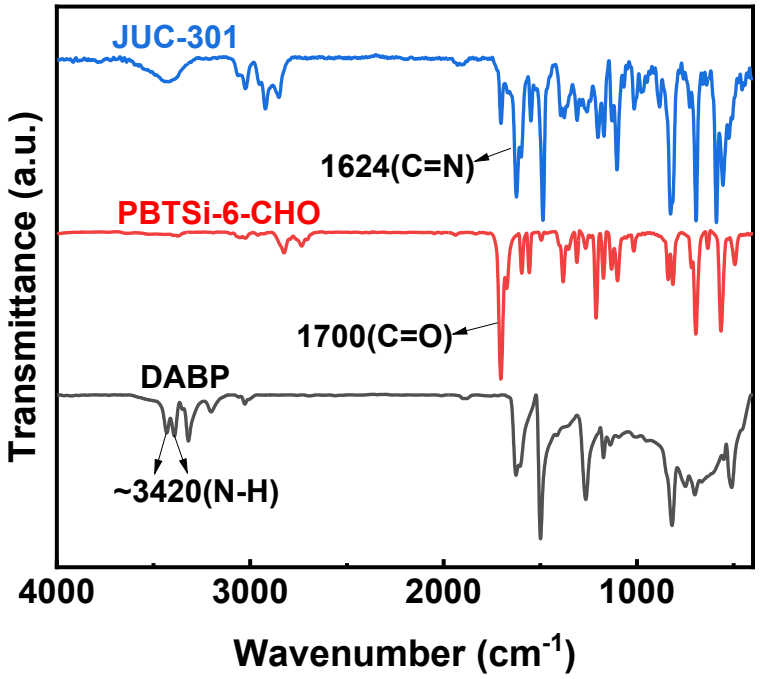

Figure S4. FT-IR spectra of DABP, PBTSi-6-CHO and JUC-301.

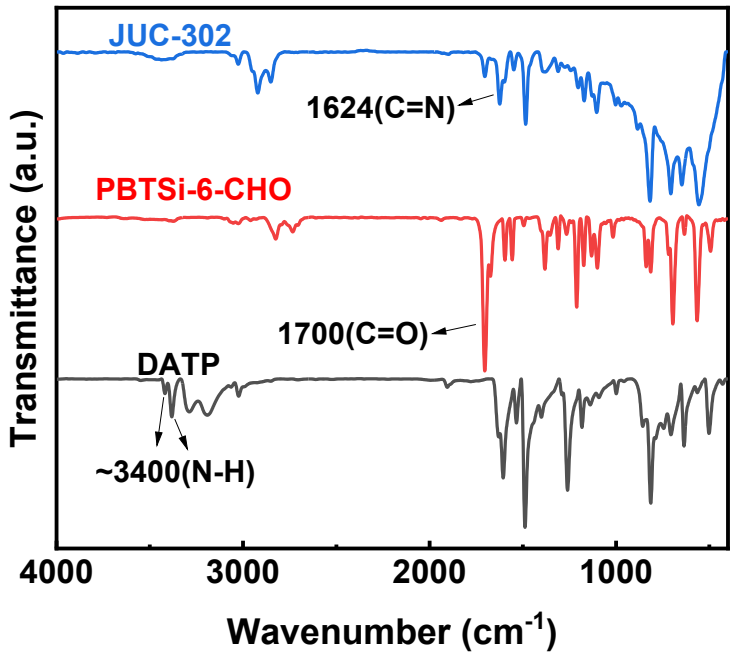

Figure S5. FT-IR spectra of DATP, PBTSi-6-CHO and JUC-302.

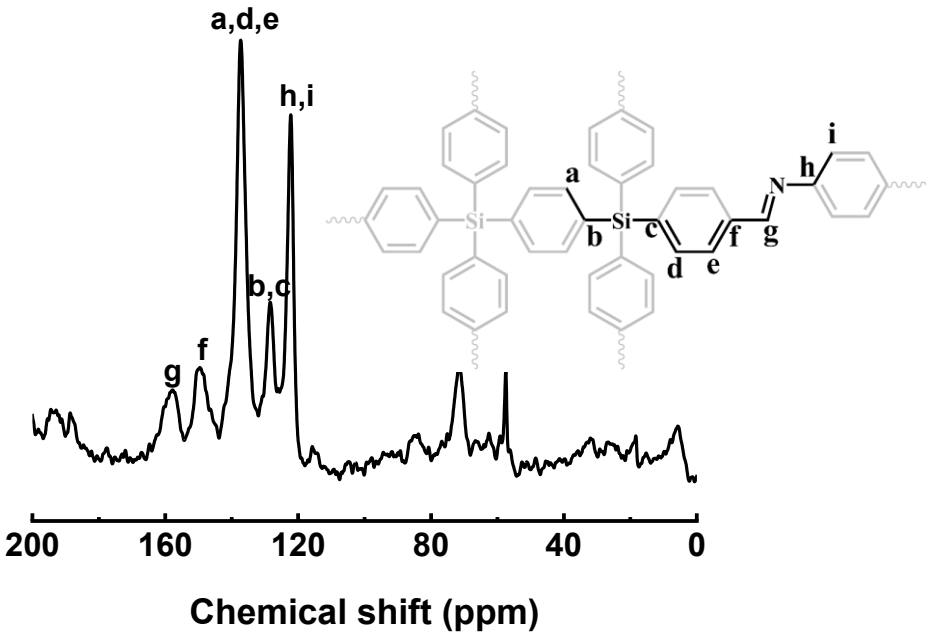

Figure S6. Solid state ^{13}C NMR of JUC-300.

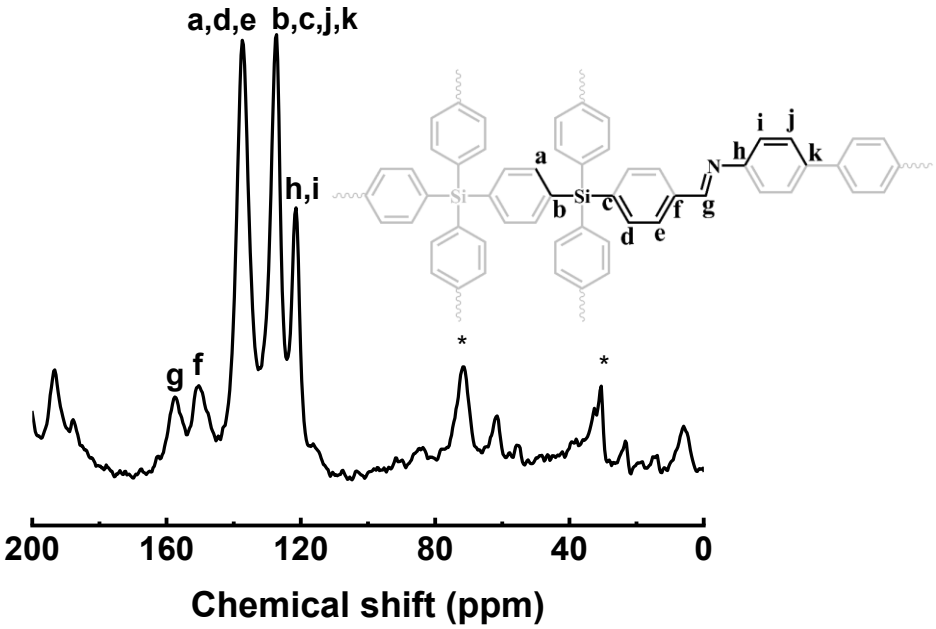

Figure S7. Solid state ^{13}C NMR of JUC-301.

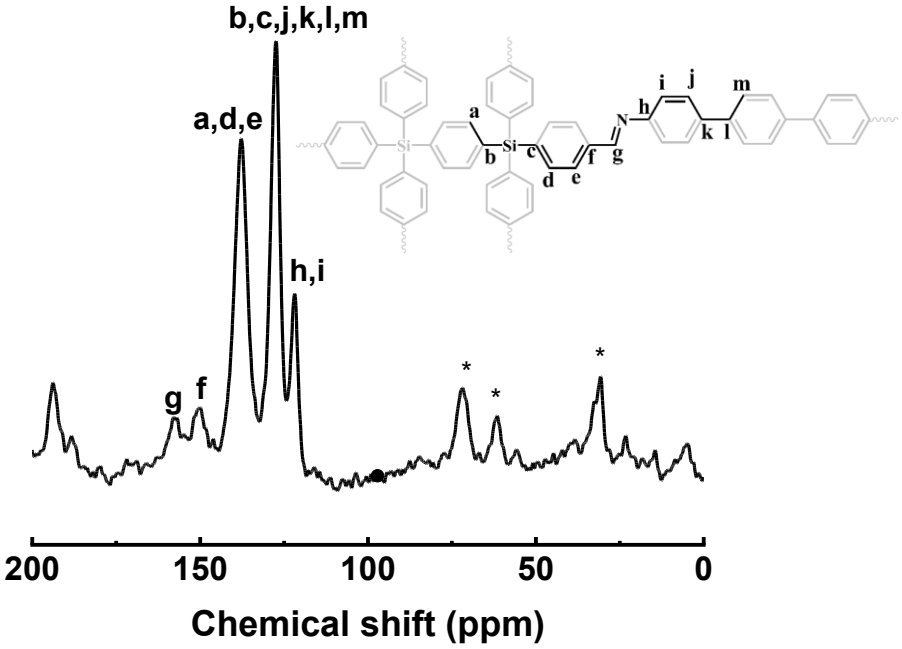

Figure S8. Solid state ^{13}C NMR of JUC-302.

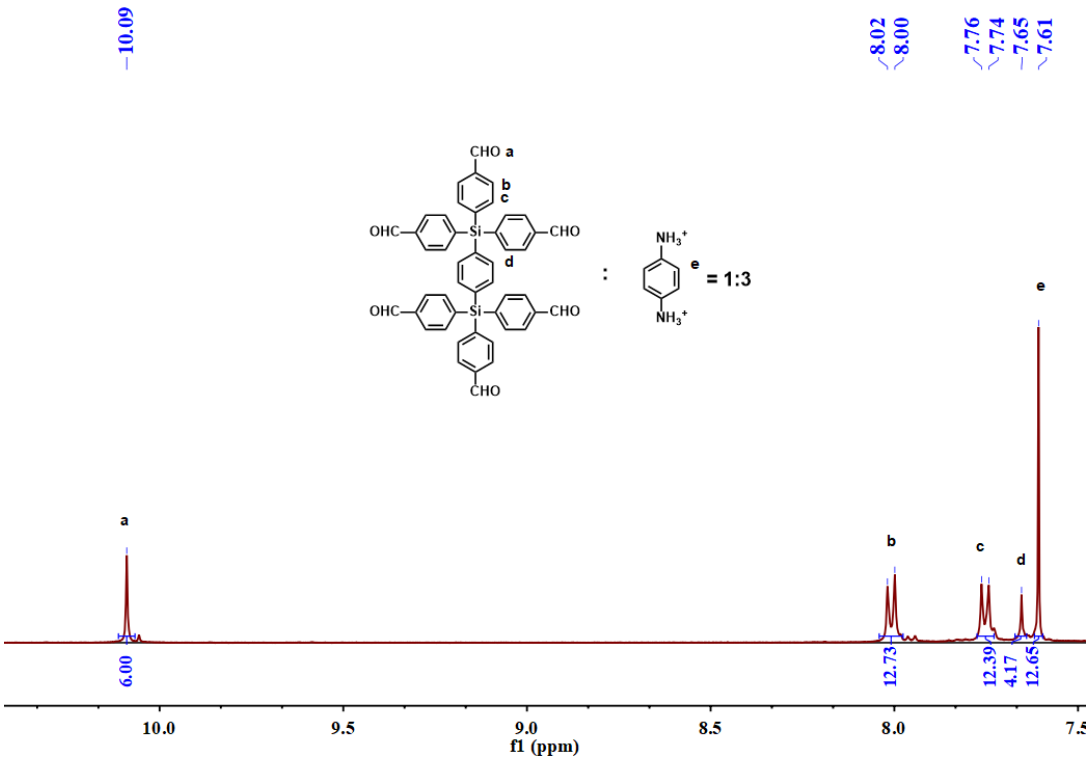

Figure S9. [1]H NMR spectrum of the acid digested JUC-300. The linker ratio of PBTSi-6CHO to PPDA is ~1:3.

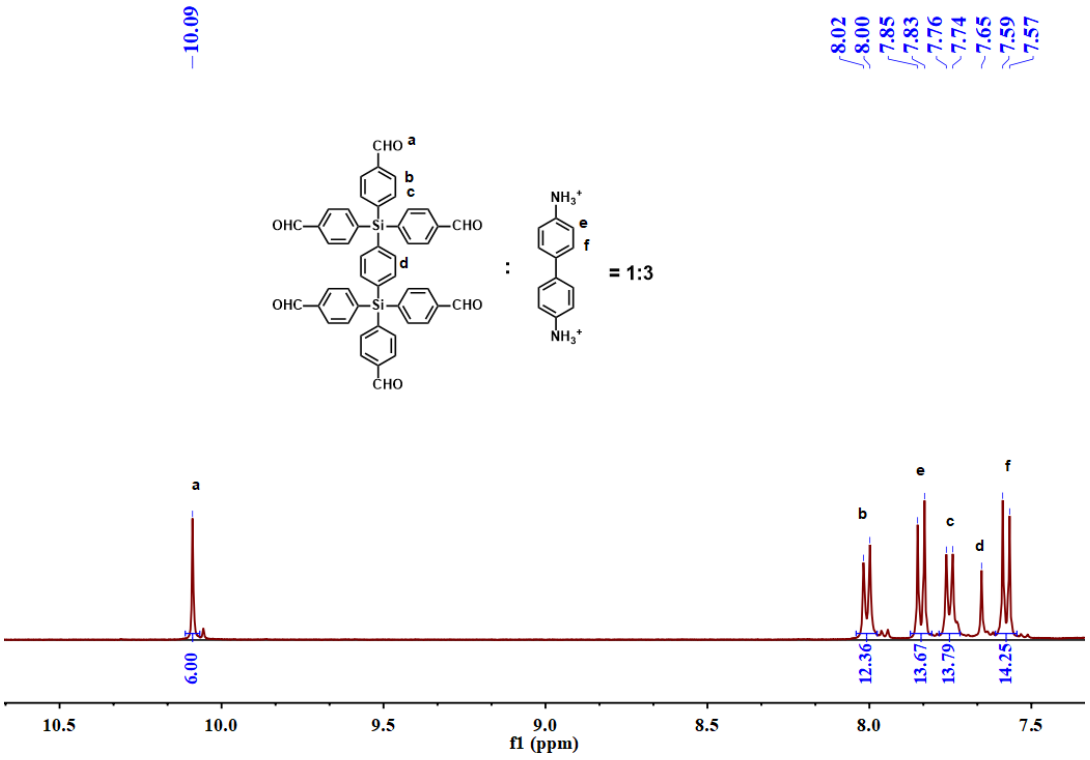

Figure S10. [1]H NMR spectrum of the acid digested JUC-301. The linker ratio of PBTSi-6CHO to DABP is ~1:3.

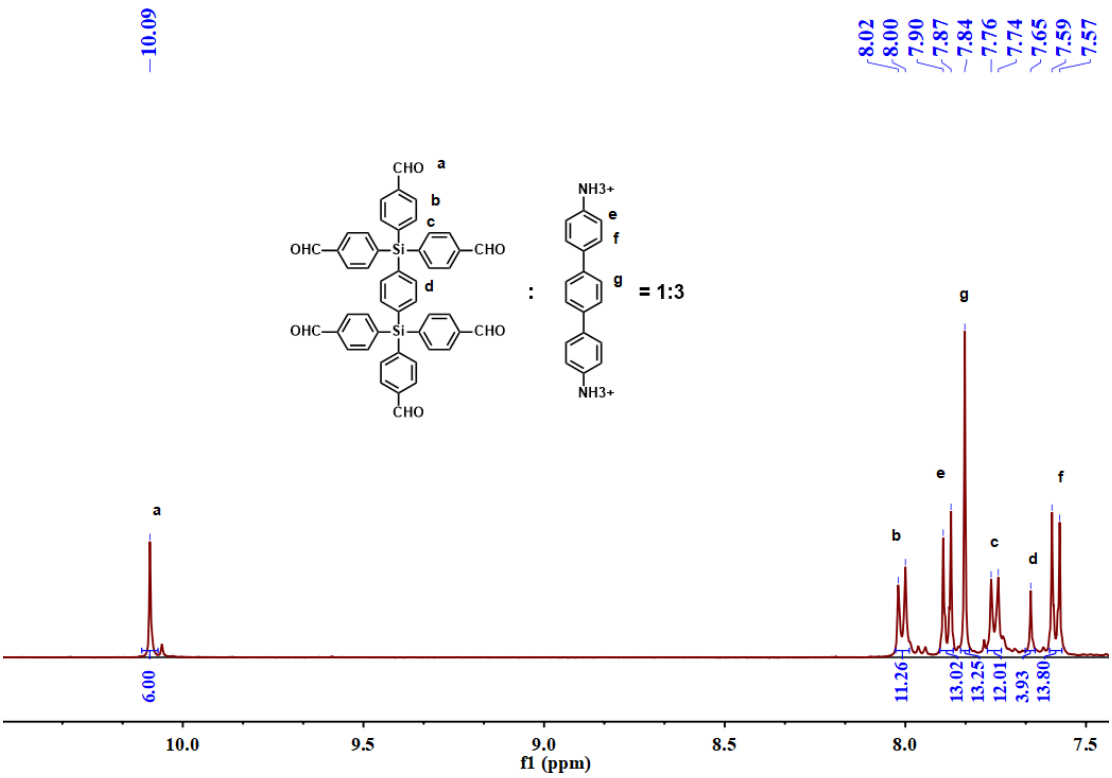

Figure S11. [1]H NMR spectrum of the acid digested JUC-302. The linker ratio of PBTSi-6CHO to DATP is ~1:3.

Section S5. TGA curves

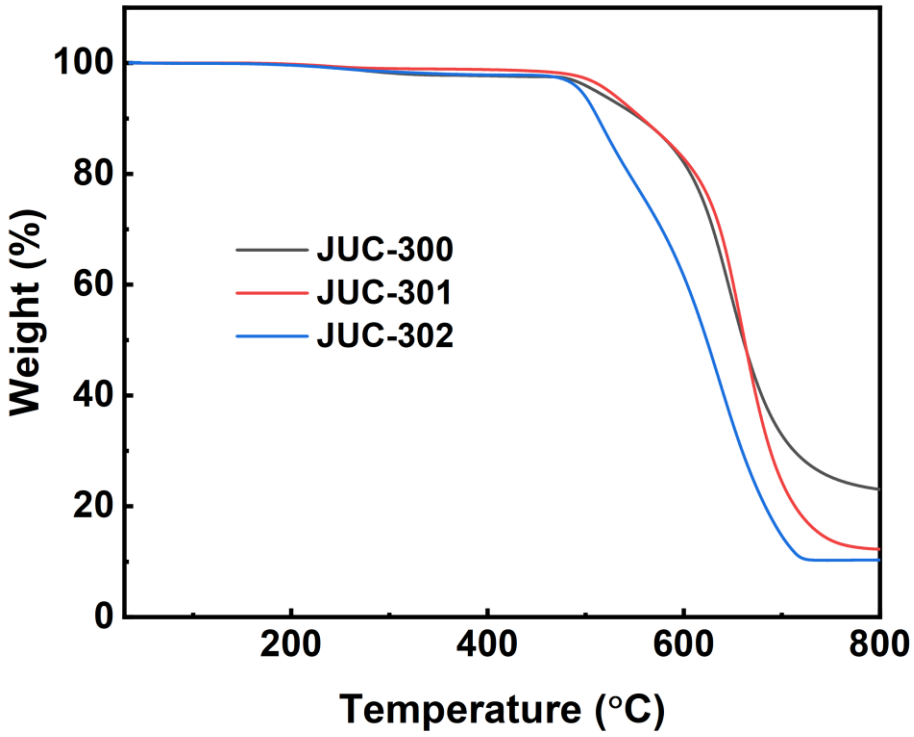

Figure S12. TG curves of JUC-300 (black), JUC-301 (red), JUC-302 (blue).

Section S6. SEM and TEM images

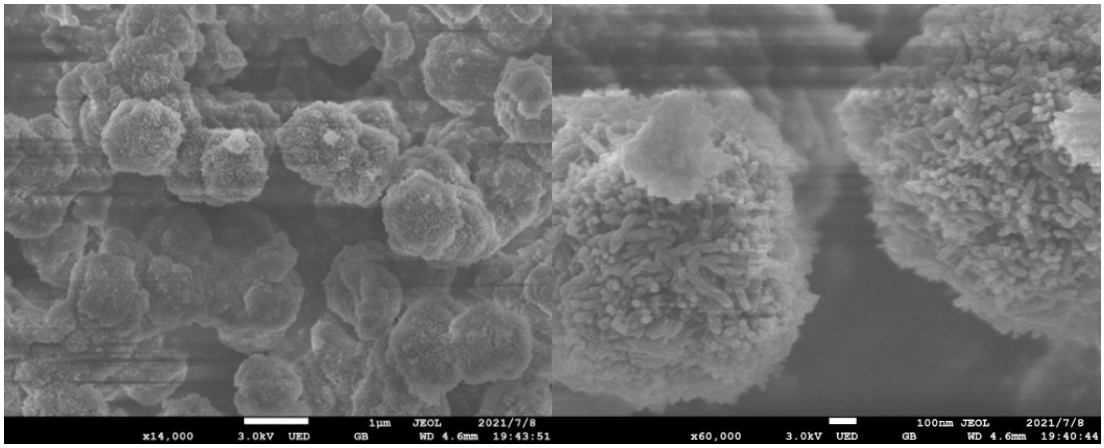

Figure S13. SEM images of JUC-300 on a Si wafer.

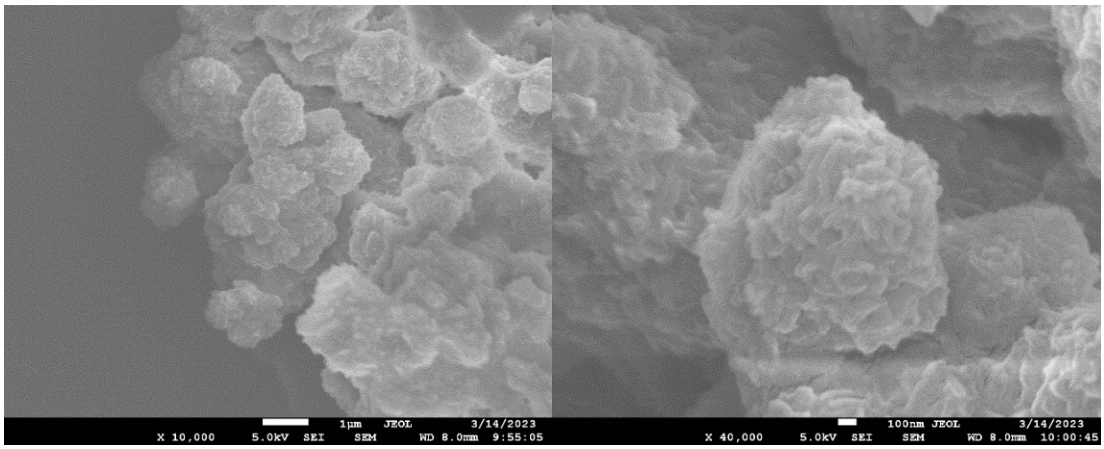

Figure S14. SEM images of JUC-301 on a Si wafer.

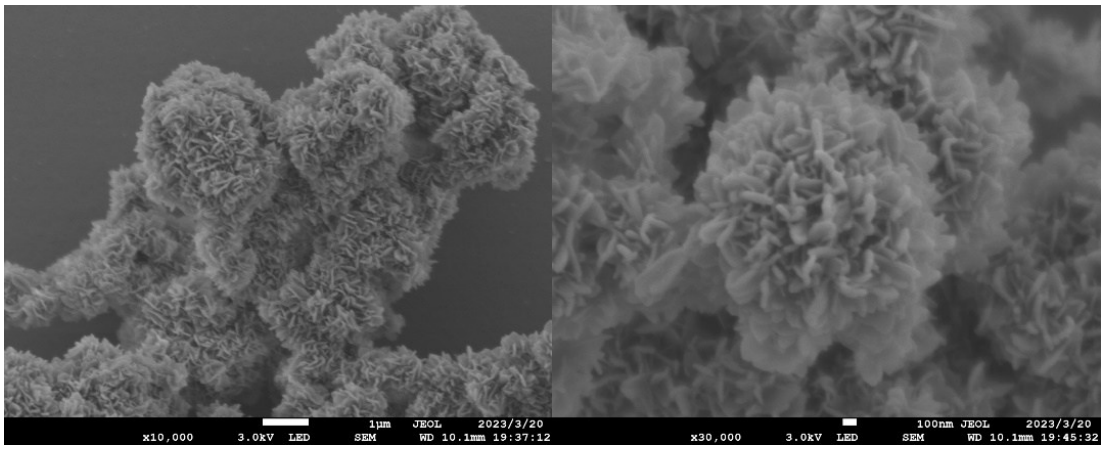

Figure S15. SEM images of JUC-302 on a Si wafer.

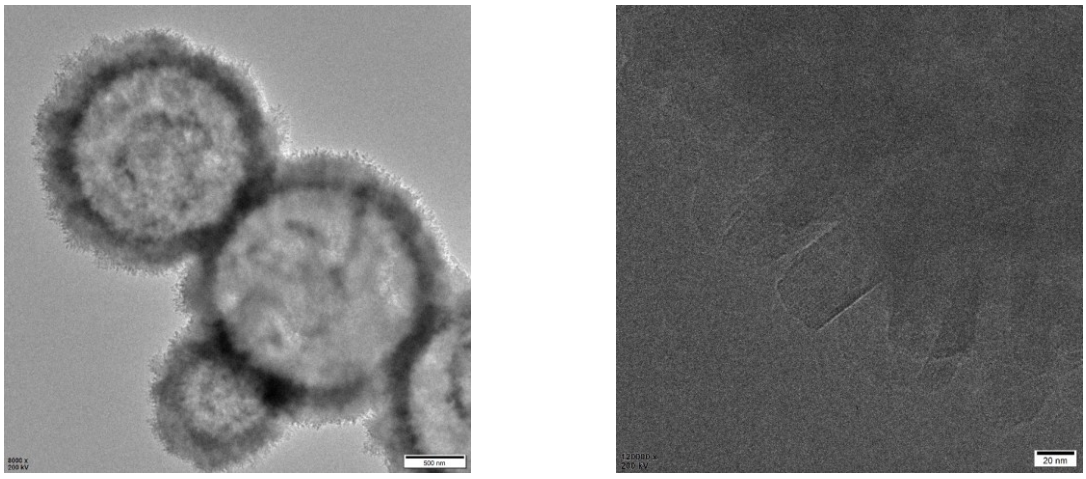

Figure S16. TEM images of the JUC-300.

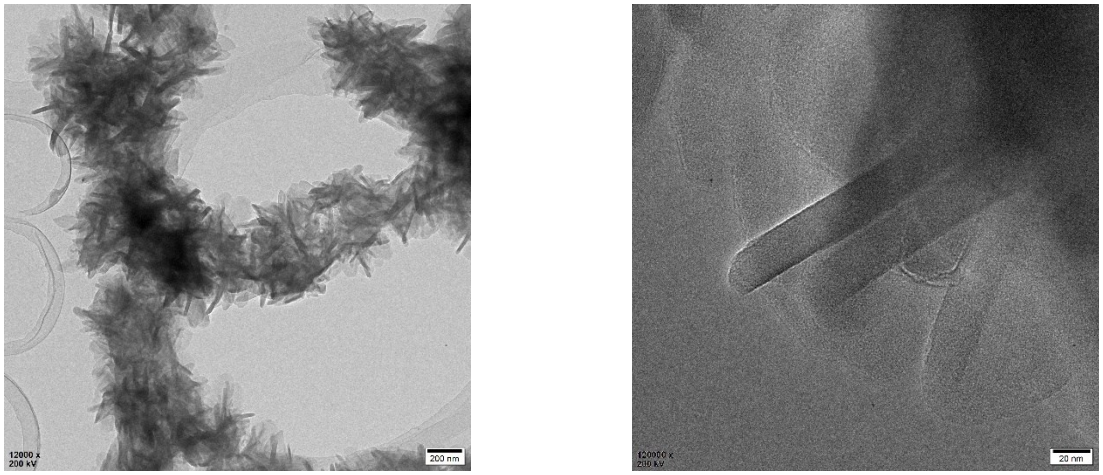

Figure S17. TEM images of the JUC-301.

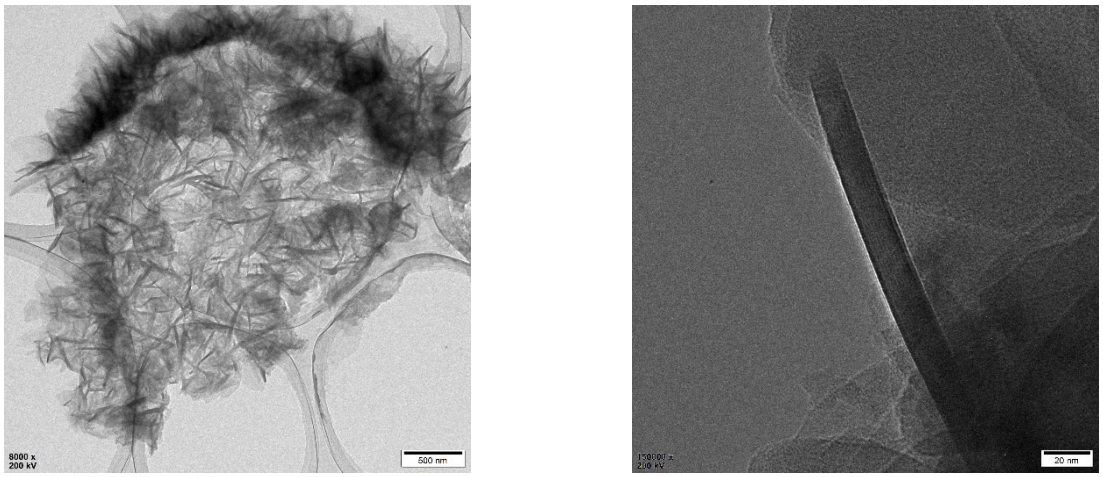

Figure S18. TEM images of the JUC-302.

Section S7. Structural models

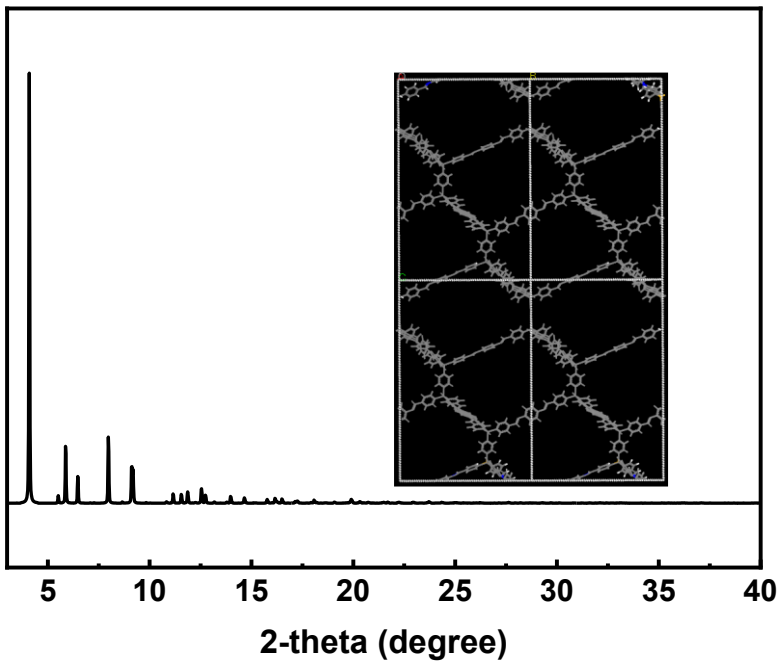

Figure S19. Calculated PXRD pattern of JUC-300 based on the non-interpenetrated distorted **dia** net.

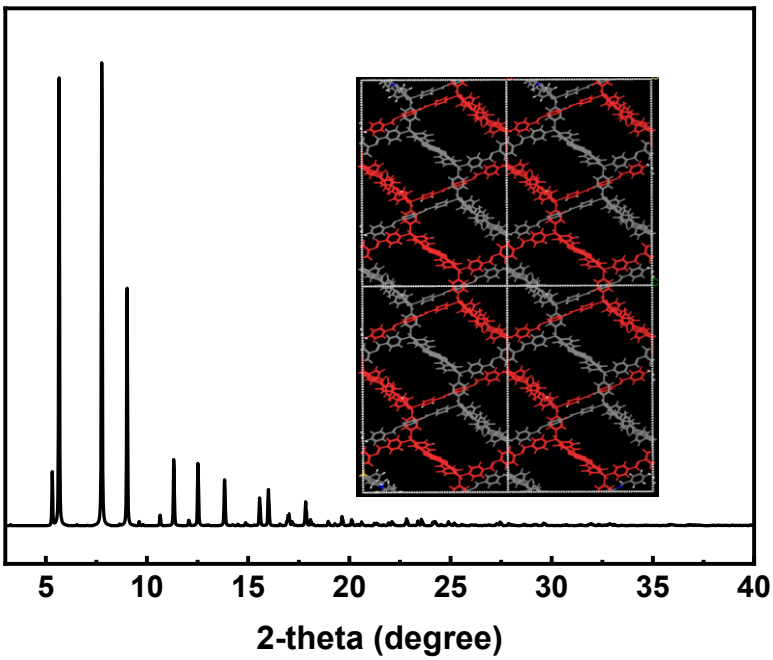

Figure S20. Calculated PXRD pattern of JUC-300 based on the 2-fold interpenetrated distorted dia net.

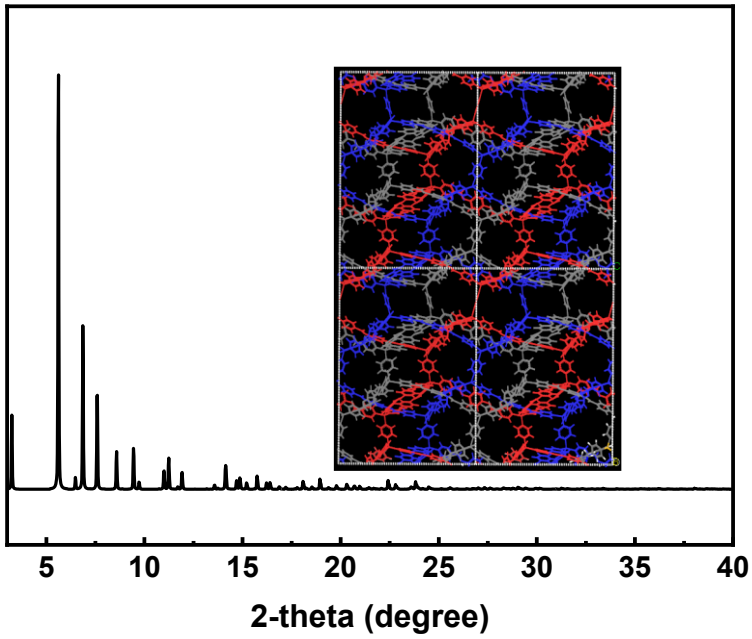

Figure S21. Calculated PXRD pattern of JUC-300 based on the 3-fold interpenetrated distorted **dia** net.

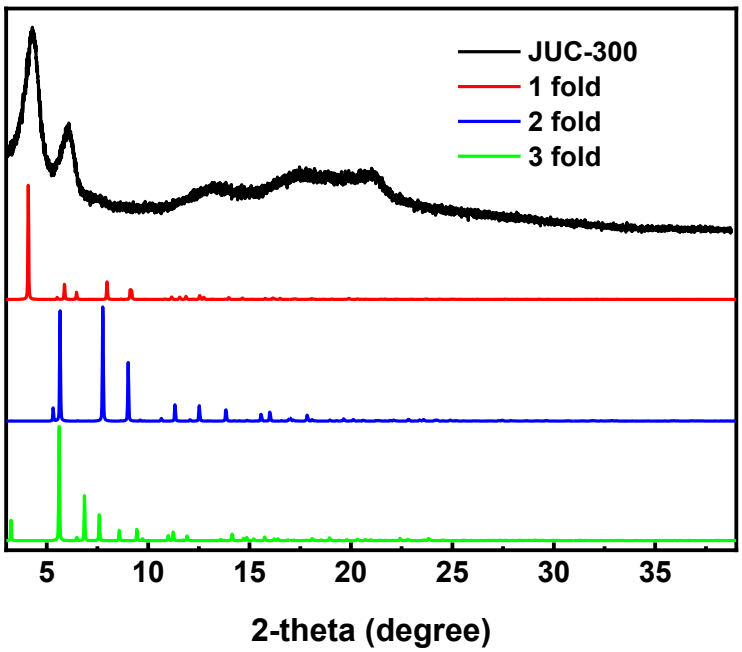

Figure S22. Comparison of PXRD patterns for JUC-300: experimental (black) as well as calculated from the non-, 2-fold and 3-fold interpenetrated distorted **dia** nets.

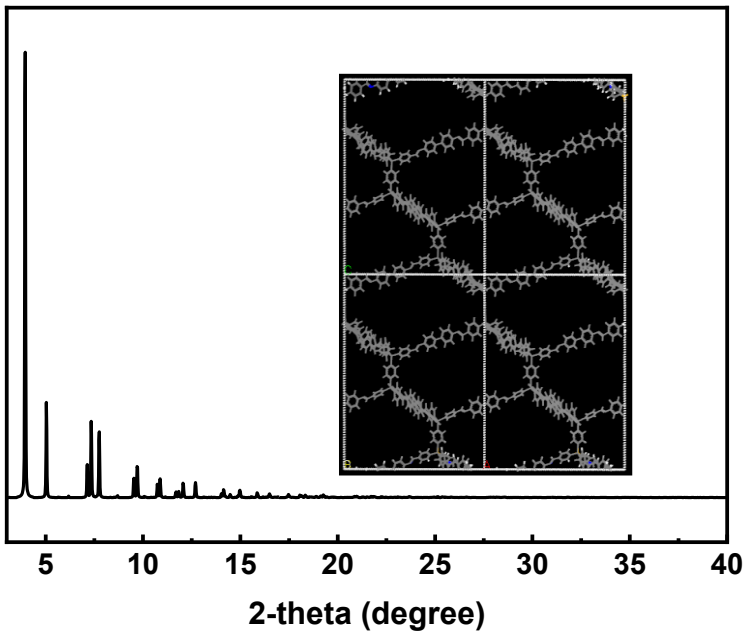

Figure S23. Calculated PXRD pattern of JUC-301 based on the non-interpenetrated distorted dia net.

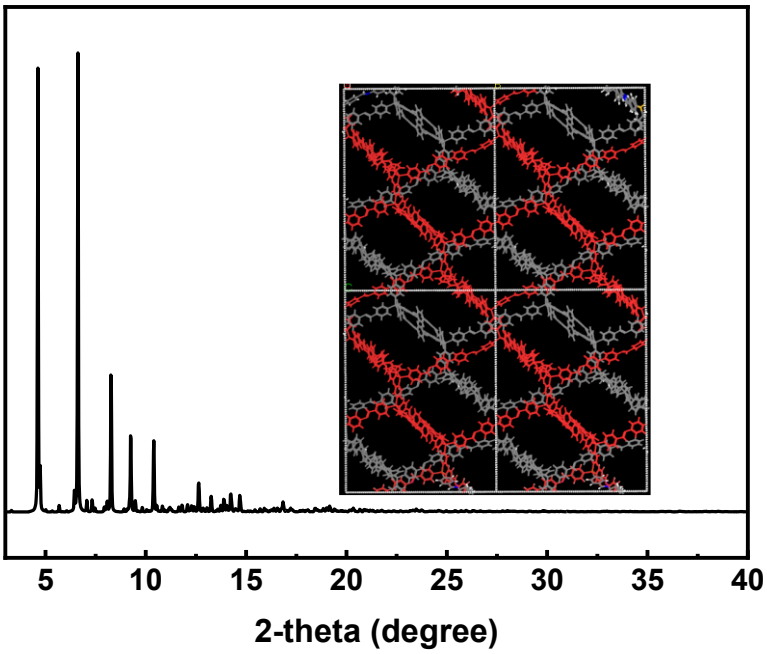

Figure S24. Calculated PXRD pattern of JUC-301 based on the 2-fold interpenetrated distorted dia net.

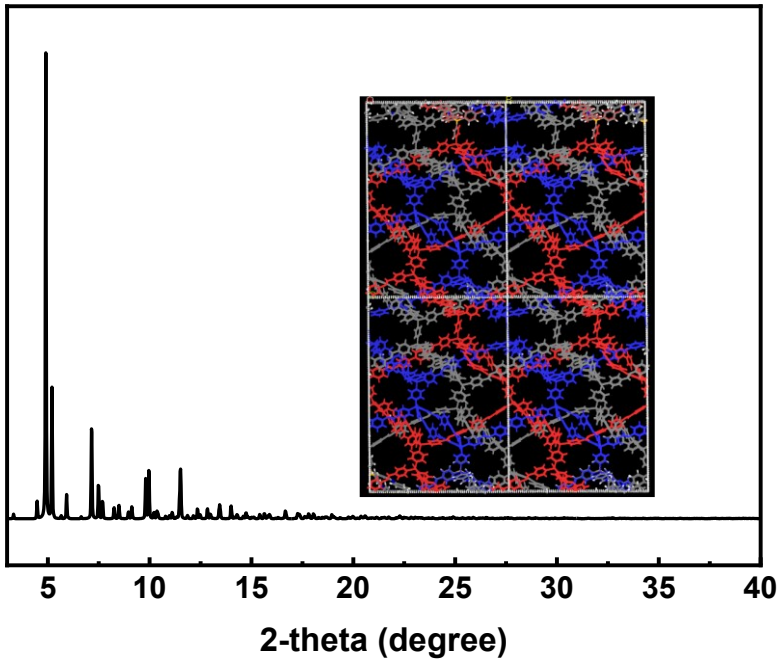

Figure S25. Calculated PXRD pattern of JUC-301 based on the 3-fold interpenetrated distorted dia net.

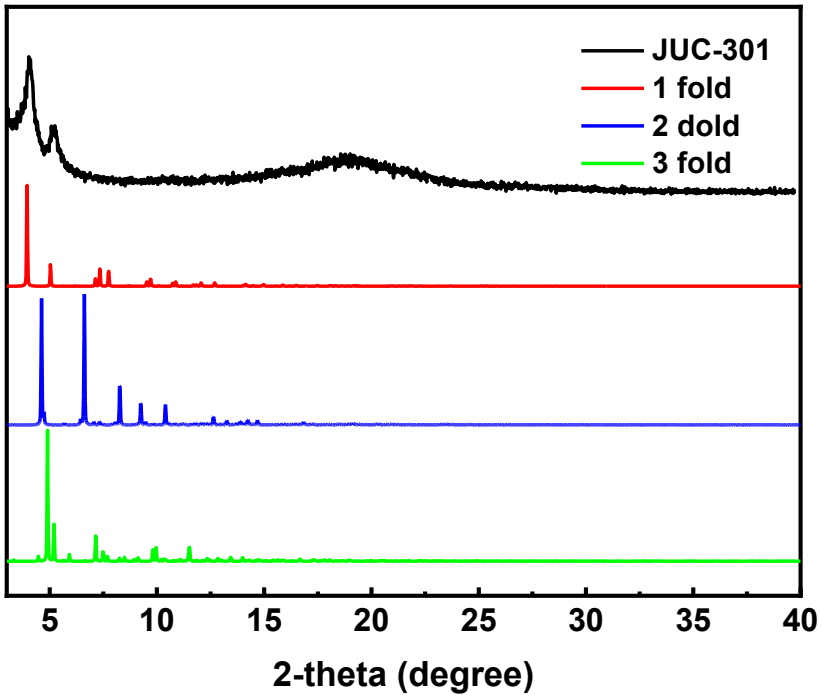

Figure S26. Comparison of PXRD patterns for JUC-301: experimental (black) as well as calculated from the non-, 2-fold and 3-fold interpenetrated distorted dia nets.

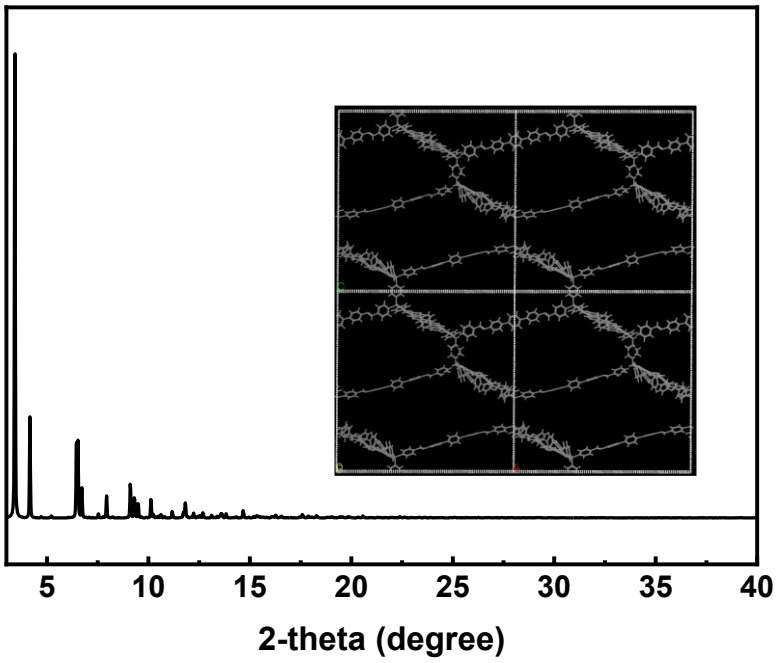

Figure S27. Calculated PXRD pattern of JUC-302 based on the non-interpenetrated distorted dia net.

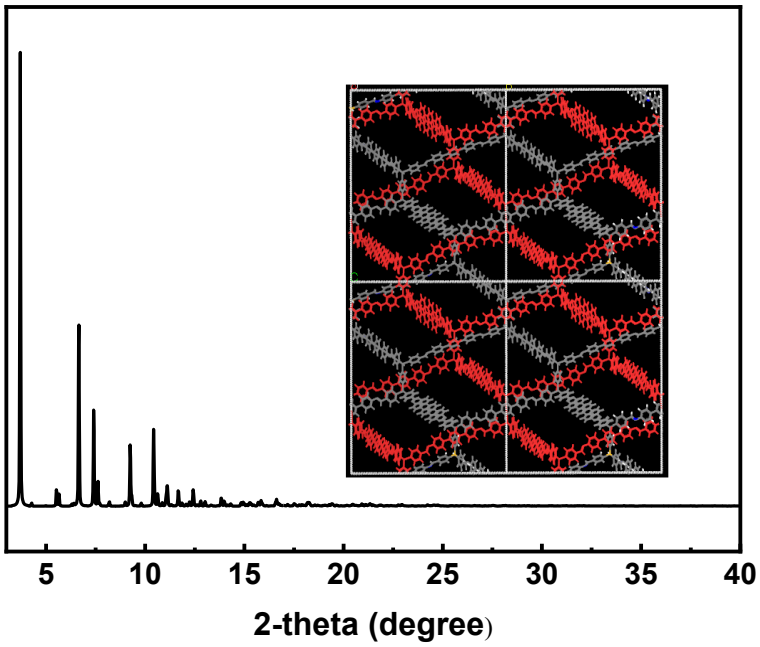

Figure S28. Calculated PXRD pattern of JUC-302 based on the 2-fold interpenetrated distorted dia net.

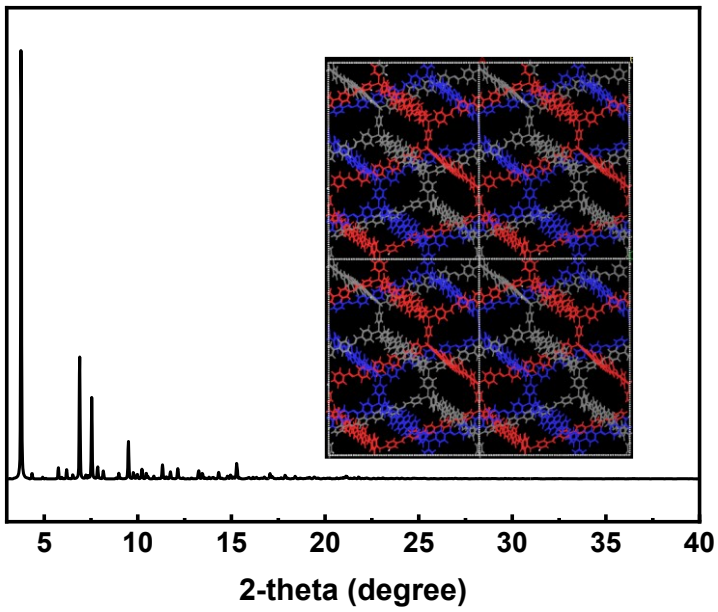

Figure S29. Calculated PXRD pattern of JUC-302 based on the 3-fold interpenetrated distorted dia net.

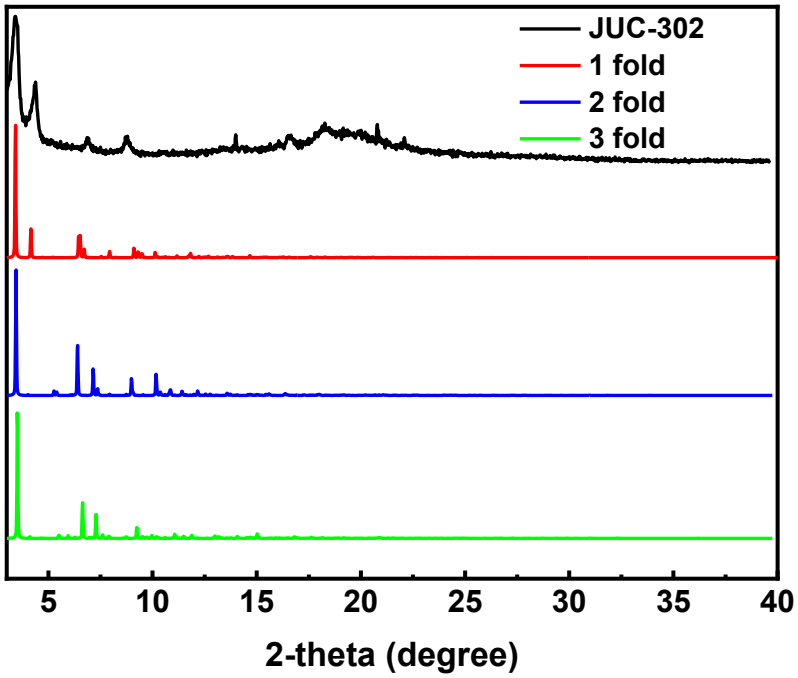

Figure S30. Comparison of PXRD patterns for JUC-302: experimental (black) as well as calculated from the non-, 2-fold and 3-fold interpenetrated distorted dia nets.

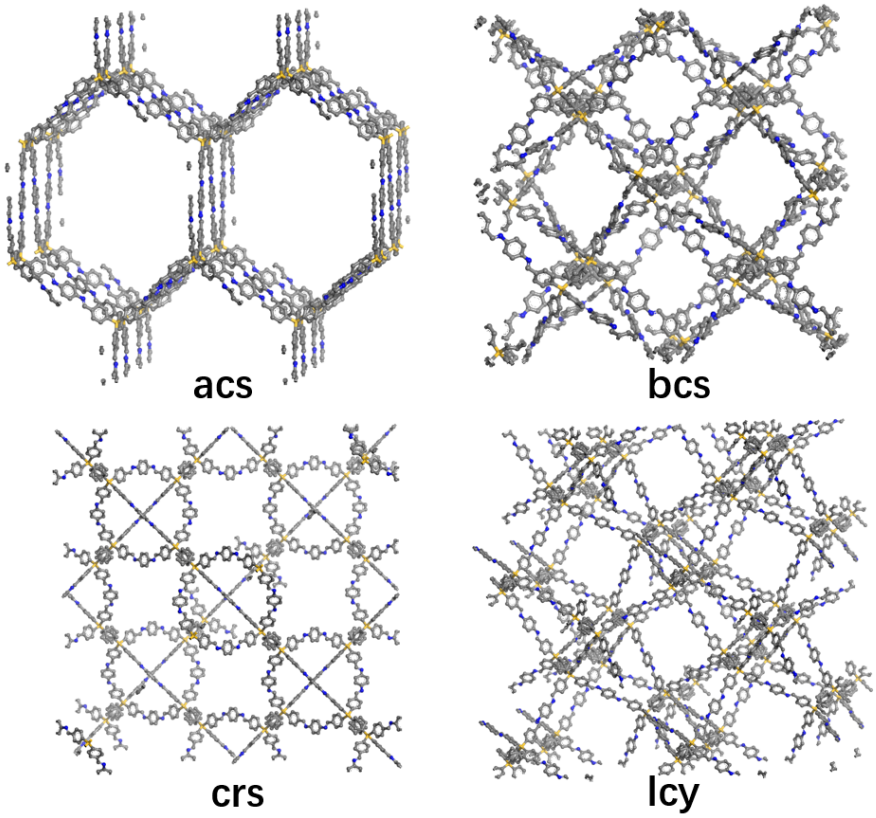

Figure S31. The structural models of JUC-300 with different topologies

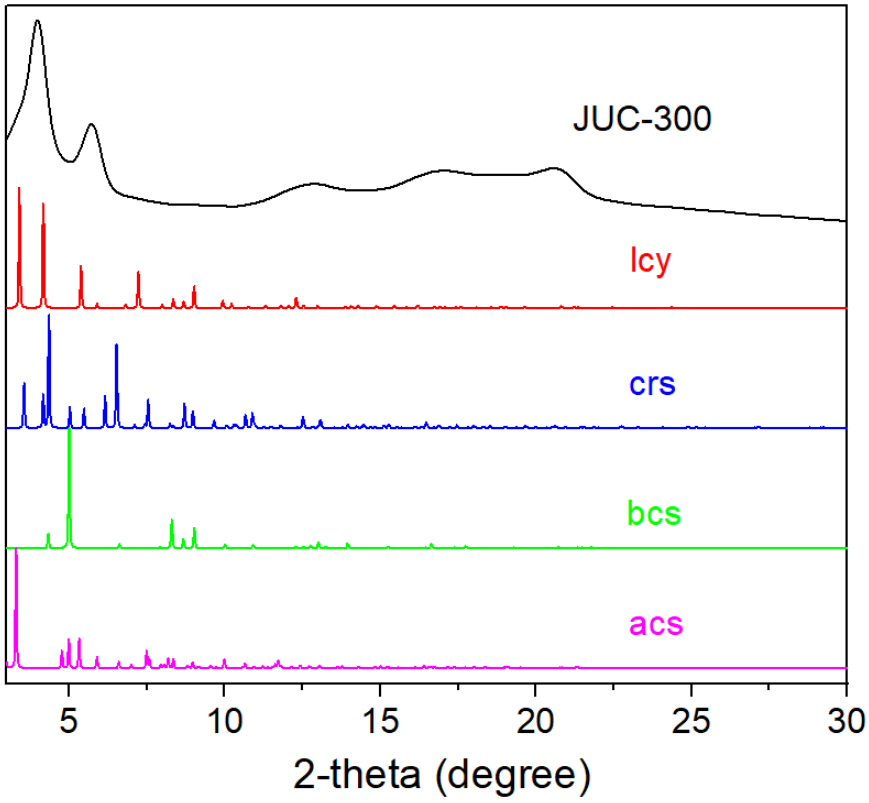

Figure S32. Comparison of PXRD patterns for JUC-300: experimental (black) as well as calculated from the structural models with different topologies.

Table S2. Unit cell parameters and fractional atomic coordinates for JUC-300 calculated based on the non-interpenetrated distorted dia net.

Space group		$P3_221$ (No.154)	
Calculated unit cell		$a = b = 31.33434$ Å, $c = 41.61373$ Å $\alpha = \beta = 90^o$, $\gamma = 120^o$	
Atoms	X	Y	Z
C1	0.2979	0.2969	0.5165
C2	0.3756	0.3742	0.5164
C3	0.9109	0.6595	0.7529
C4	0.8625	0.6406	0.7419
C5	0.9238	0.6088	0.7151
C6	0.6941	0.5455	0.6751
C7	0.646	0.5204	0.6629
C8	0.8441	0.605	0.7177
C9	0.8753	0.5897	0.7042
C10	0.7923	0.584	0.7071
N11	0.577	0.4446	0.6382
C12	0.7231	0.5225	0.6757
C13	0.3254	0.2363	0.5736
C14	0.3056	0.1869	0.5829
C15	0.2815	0.2492	0.6164
C16	0.1857	0.0091	0.6341
C17	0.161	-0.0396	0.6455
C18	0.2739	0.1683	0.609
C19	0.2622	0.2	0.6259
C20	0.2526	0.1158	0.6181
N21	0.2295	0.0996	0.6448
C22	0.206	0.0491	0.6554
C23	0.4272	0.4238	0.5896
C24	0.4753	0.4533	0.601
C25	0.4283	0.3502	0.6066
C26	0.6552	0.4494	0.6515
C27	0.7034	0.4746	0.6636
C28	0.5005	0.4316	0.6151
C29	0.4766	0.3798	0.6179
C30	0.5513	0.4636	0.627
N31	0.7728	0.5467	0.6877
C32	0.6263	0.4721	0.6507
C33	0.4033	0.372	0.5923
C34	0.2985	0.3569	0.5933
C35	0.3131	0.2676	0.5902
Si36	0.3385	0.3331	0.5773

C37	0.3373	0.335	0.5333
H38	0.2679	0.266	0.5289
H39	0.4068	0.4041	0.5285
H40	0.924	0.6865	0.7718
H41	0.8391	0.6532	0.7525
H42	0.9471	0.5967	0.7039
H43	0.7086	0.5829	0.6836
H44	0.6241	0.5385	0.6634
H45	0.8621	0.5628	0.6852
H46	0.3499	0.2499	0.5534
H47	0.3151	0.1631	0.5696
H48	0.2717	0.2728	0.6297
H49	0.1875	0.0154	0.609
H50	0.1449	-0.0703	0.6291
H51	0.2378	0.1863	0.6461
H52	0.2578	0.0913	0.6024
H53	0.4083	0.4415	0.579
H54	0.4929	0.4931	0.5987
H55	0.4107	0.3104	0.6092
H56	0.6402	0.4122	0.6424
H57	0.7256	0.4568	0.6638
H58	0.4954	0.3624	0.6288
H59	0.5672	0.5033	0.6253
H60	0.7704	0.5989	0.7169

Table S3. Unit cell parameters and fractional atomic coordinates for JUC-301 calculated based on the non-interpenetrated dia net.

Space group		$P3_221$ (No.154)	
Calculated unit cell		$a = b$ = 39.3180 Å, c=39.6526 Å $\alpha = \beta$ = 90º, γ = 120º	
Atoms	X	Y	Z
C1	0.3013	0.303	0.4825
C2	0.3628	0.3641	0.4825
C3	0.3776	0.3012	0.4199
C4	0.3972	0.2835	0.4056
C5	0.3594	0.3118	0.3646
C6	0.398	0.2797	0.3705
C7	0.3791	0.2943	0.3502
C8	0.4178	0.2605	0.3548
N9	0.5691	0.099	0.3026
C10	0.2588	0.2679	0.4038
C11	0.2208	0.2465	0.391
C12	0.2633	0.3279	0.3836
C13	0.2038	0.2657	0.3742
C14	0.2256	0.3065	0.3703
C15	0.1637	0.244	0.3606
N16	0.1395	0.2083	0.37
C17	0.6631	0.0745	0.2452
C18	0.6468	0.098	0.2526
C19	0.6148	0.0232	0.2806
C20	0.6145	0.0844	0.2741
C21	0.5985	0.0467	0.2881
C22	0.598	0.1099	0.2816
N23	0.4338	0.2449	0.373
C24	0.3526	0.3897	0.4073
C25	0.3586	0.3154	0.3995
C26	0.2799	0.3088	0.4009
Si27	0.3305	0.337	0.4182
C28	0.3313	0.3343	0.4648
C29	0.5504	0.121	0.3116
C30	0.5276	0.1104	0.3408
C31	0.5086	0.1307	0.3506
C32	0.5119	0.1619	0.3312
C33	0.5343	0.1722	0.3017
C34	0.5534	0.1519	0.2919
C35	0.4917	0.1835	0.3415
C36	0.4727	0.1944	0.3177

C37	0.4536	0.2146	0.3274
C38	0.4533	0.2245	0.3613
C39	0.4721	0.2134	0.3851
C40	0.4911	0.1931	0.3754
C41	0.0998	0.1856	0.3584
C42	0.0885	0.1908	0.3262
C43	0.0494	0.1691	0.3162
C44	0.0209	0.142	0.3382
C45	0.0325	0.1362	0.37
C46	0.0717	0.1575	0.3798
H47	0.2766	0.2796	0.4697
H48	0.3865	0.3884	0.4694
H49	0.3772	0.3034	0.447
H50	0.4115	0.2725	0.4219
H51	0.3445	0.3224	0.3485
H52	0.3792	0.2917	0.3232
H53	0.4186	0.2596	0.3277
H54	0.2716	0.2525	0.416
H55	0.2049	0.215	0.3939
H56	0.2792	0.3592	0.38
H57	0.2132	0.3218	0.3572
H58	0.154	0.2593	0.3441
H59	0.688	0.0856	0.2284
H60	0.6595	0.1269	0.2414
H61	0.6018	-0.0058	0.2914
H62	0.5735	0.0353	0.3046
H63	0.6112	0.1384	0.2698
H64	0.5246	0.0863	0.356
H65	0.491	0.1216	0.3732
H66	0.5375	0.1962	0.2862
H67	0.5697	0.1604	0.2687
H68	0.4721	0.1868	0.2915
H69	0.4389	0.2218	0.3082
H70	0.472	0.2206	0.4113
H71	0.5058	0.1854	0.3943
H72	0.1098	0.2114	0.3087
H73	0.0412	0.1741	0.2916
H74	0.0111	0.1151	0.3873
H75	0.0801	0.1528	0.4045

Table S4. Unit cell parameters and fractional atomic coordinates for JUC-302 calculated based on the non-interpenetrated dia net.

Space group		$P3_221$ (No.154)	
Calculated unit cell		$a = b = 46.8052$ Å, $c = 41.8554$ Å $\alpha = \beta = 90^o$, $\gamma = 120^o$	
Atoms	X	Y	Z
Si1	-0.0004	0.6687	0.2553
C2	0.0006	0.6691	0.2997
C3	-0.0003	0.6945	0.3167
C4	0.0004	0.6431	0.3166
C5	0.2267	0.4285	0.1194
C6	0.2434	0.4627	0.1229
C7	0.2265	0.4791	0.1315
C8	0.1921	0.4613	0.1363
C9	0.1752	0.4269	0.1321
C10	0.1923	0.4106	0.1238
C11	0.1741	0.4787	0.1456
C12	0.1485	0.4648	0.1683
C13	0.1322	0.4816	0.1777
C14	0.1413	0.5128	0.1648
C15	0.1667	0.5265	0.142
C16	0.1828	0.5097	0.1324
C17	0.1248	0.5311	0.1755
C18	0.1435	0.5649	0.1826
C19	0.128	0.5822	0.193
C20	0.0937	0.5663	0.196
C21	0.0749	0.5324	0.1892
C22	0.0903	0.515	0.1791
N23	0.0792	0.5853	0.2071
C24	0.0487	0.5779	0.203
C25	0.0369	0.5996	0.2158
N26	0.2456	0.413	0.1108
C27	0.2367	0.3821	0.1147
C28	0.2588	0.3697	0.1051
C29	0.0051	0.5934	0.2081
C30	-0.0063	0.6139	0.2197
C31	0.0138	0.6406	0.2396
C32	0.0455	0.6469	0.2473
C33	0.057	0.6266	0.2356
C34	0.2509	0.3374	0.1133
C35	0.2721	0.3256	0.1052
C36	0.3017	0.346	0.0889

C37	0.3091	0.3778	0.0798
C38	0.288	0.3897	0.0881
C39	0.2671	0.1364	0.1319
C40	0.2737	0.1148	0.1146
C41	0.2594	0.0816	0.1234
C42	0.2377	0.0693	0.1497
C43	0.231	0.0911	0.167
C44	0.2455	0.1243	0.1581
C45	0.2214	0.0338	0.1584
C46	0.2167	0.024	0.1906
C47	0.2	-0.0094	0.1988
N48	0.281	0.1698	0.1208
C49	0.2849	0.1948	0.1379
C50	0.2976	0.2277	0.1233
C51	0.3049	0.2329	0.0905
C52	0.3153	0.2638	0.0769
C53	0.3182	0.29	0.0957
C54	0.3124	0.2852	0.1287
C55	0.3019	0.2542	0.1423
H56	-0.001	0.7143	0.3041
H57	0.0005	0.6229	0.3041
H58	0.2699	0.4766	0.1194
H59	0.2403	0.5056	0.1349
H60	0.1487	0.4126	0.1349
H61	0.1785	0.3842	0.1201
H62	0.1416	0.4413	0.1792
H63	0.113	0.4707	0.1956
H64	0.1737	0.5502	0.1313
H65	0.202	0.5207	0.1145
H66	0.1701	0.5778	0.1806
H67	0.1426	0.6082	0.1987
H68	0.0484	0.5192	0.1923
H69	0.0753	0.4889	0.1737
H70	0.0318	0.5565	0.1892
H71	0.2137	0.3654	0.1265
H72	-0.0107	0.5728	0.1927
H73	-0.0307	0.6089	0.2128
H74	0.0616	0.6677	0.2624
H75	0.0817	0.6318	0.2418
H76	0.2283	0.3215	0.1262
H77	0.2652	0.3006	0.1116
H78	0.3315	0.3937	0.0666
H79	0.2945	0.4145	0.0812

H80	0.29	0.1239	0.0941
H81	0.2653	0.0656	0.1098
H82	0.2138	0.0822	0.1867
H83	0.2388	0.14	0.1712
H84	0.2261	0.0423	0.2095
H85	0.1961	-0.0161	0.2238
H86	0.2789	0.1919	0.1631
H87	0.3022	0.2129	0.0755
H88	0.3211	0.2671	0.0517
H89	0.3155	0.3053	0.1439
H90	0.2968	0.2509	0.1677

Section S8. Nitrogen sorptions of $ScCO_2$-activated COFs

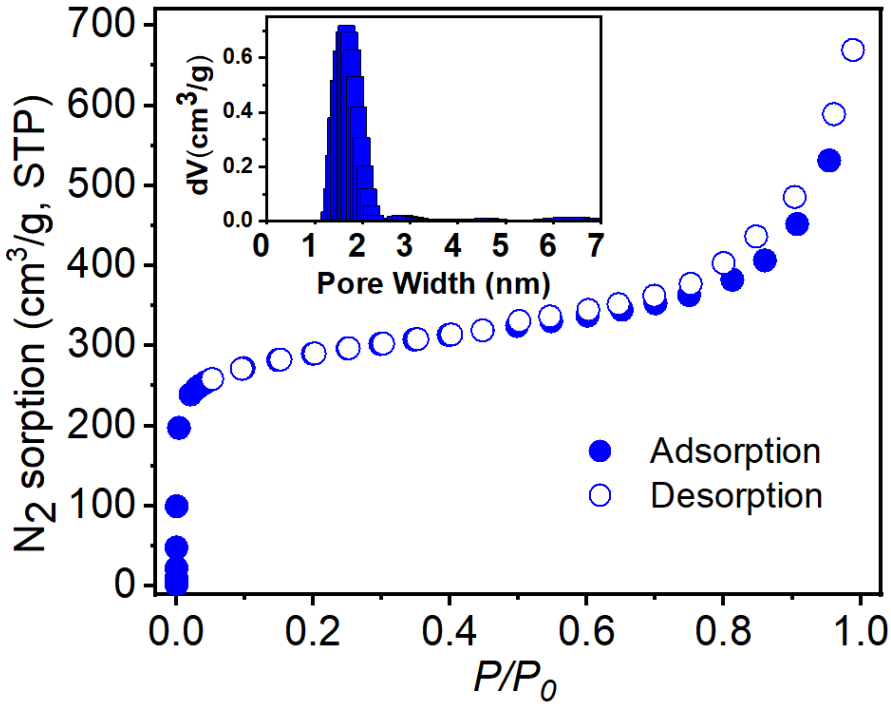

Figure S33. N_2 adsorption−desorption isotherm of JUC-300 after Sc-CO_2 activated.

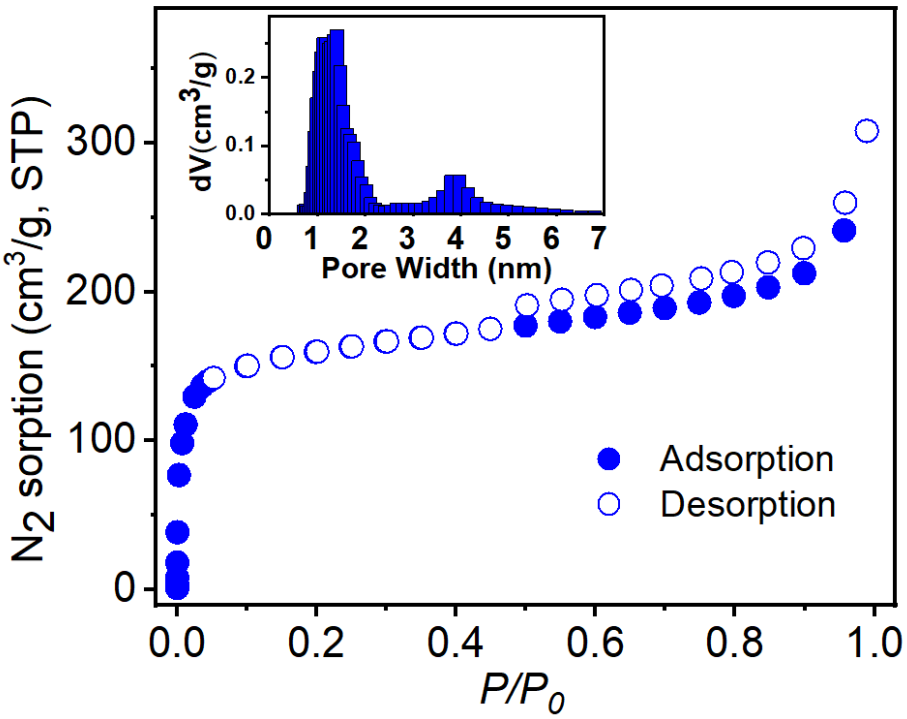

Figure S34. N_2 adsorption−desorption isotherm of JUC-301 after Sc-CO_2 activated.

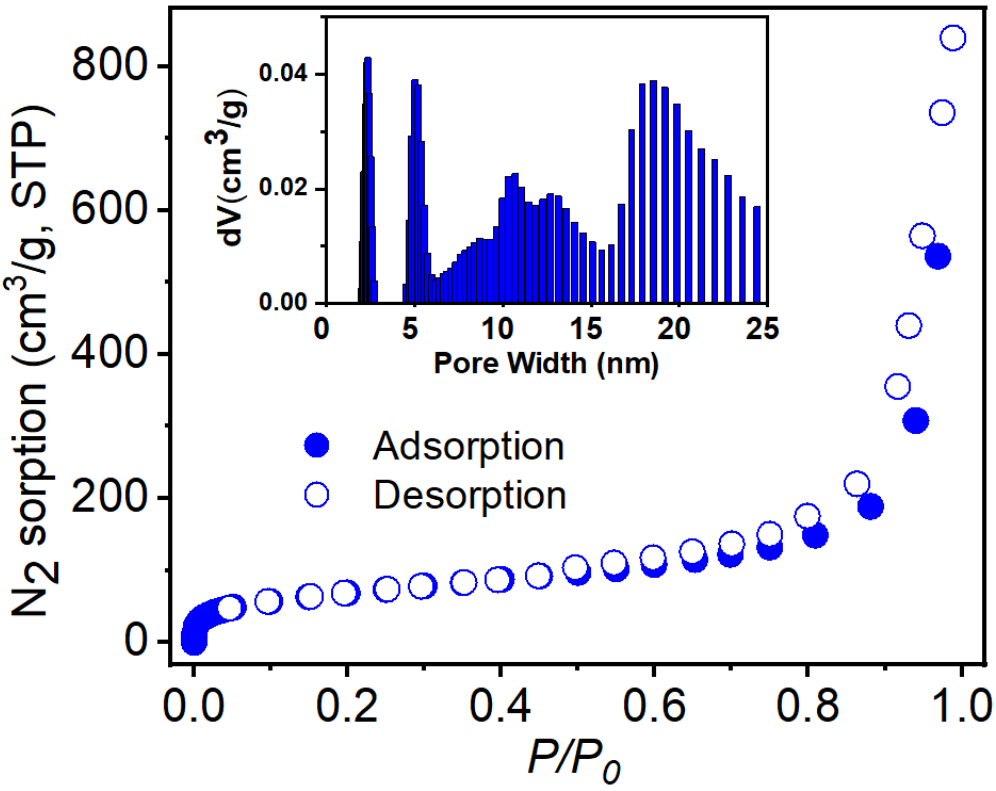

Figure S35. N_2 adsorption−desorption isotherm of JUC-302 after Sc-CO_2 activated.

Section S10. Mb concentrations

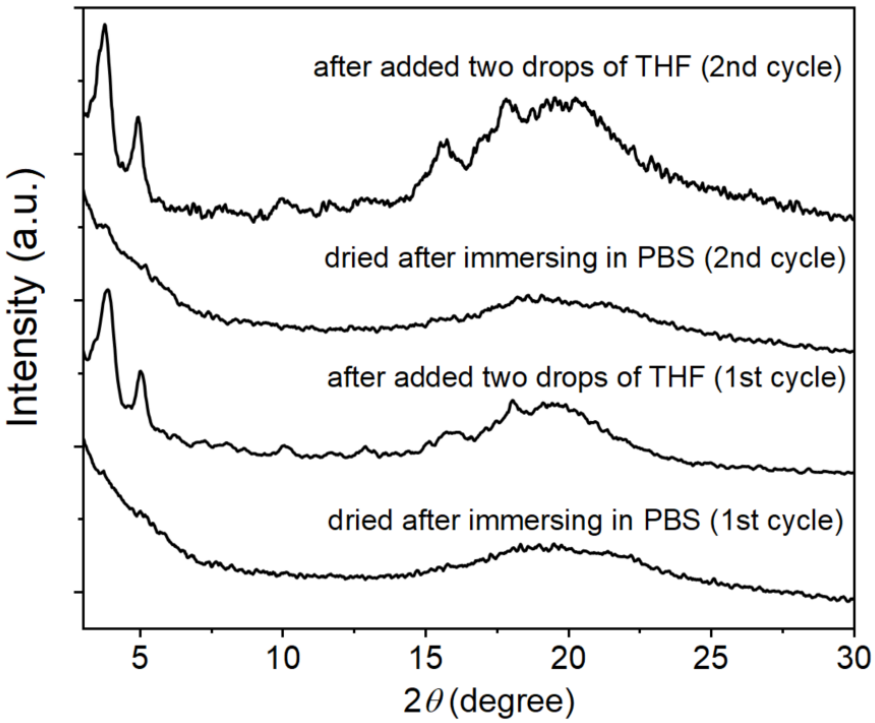

Figure S36. PXRD patterns of JUC-301 after immersing in PBS and subsequently adding THF in two cycles.

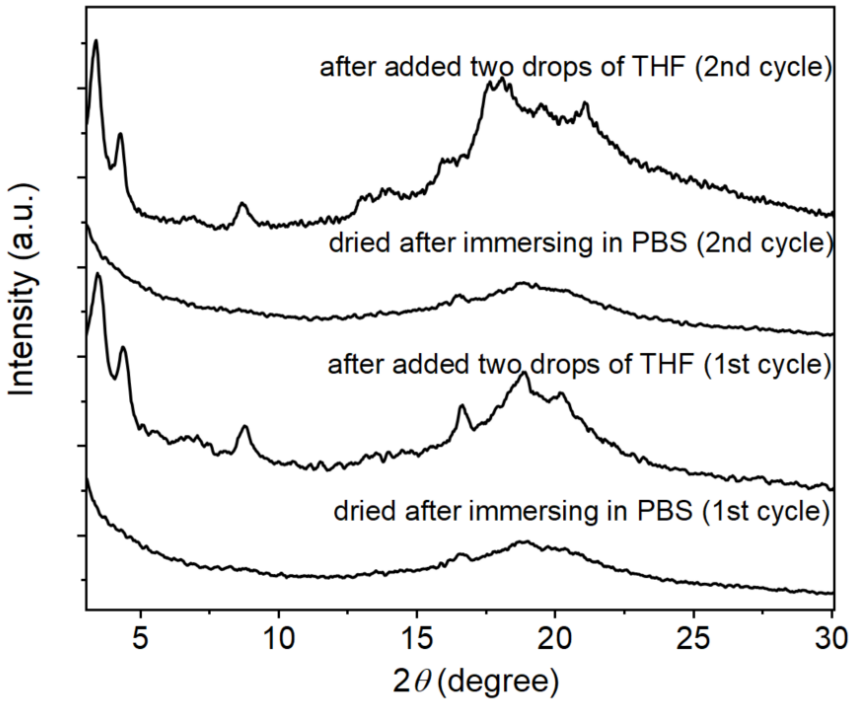

Figure S37. PXRD patterns of JUC-302 after immersing in PBS and subsequently adding THF in two cycles.

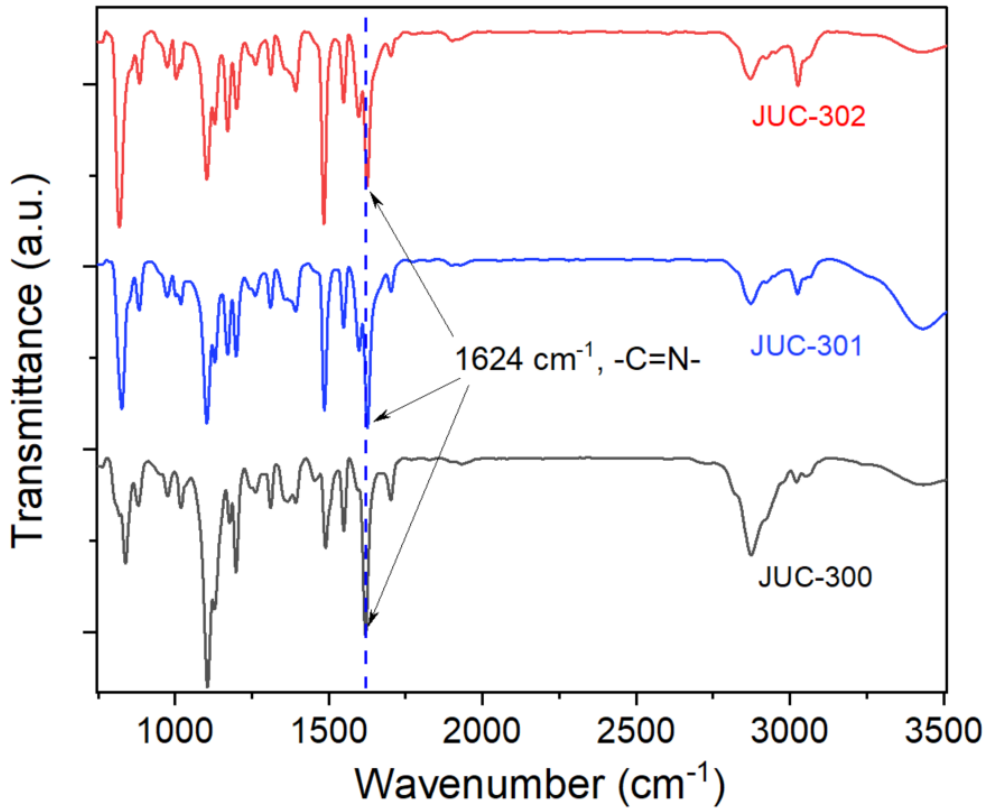

Figure S38. FT-IR spectra of JUC-300, -301 and -302 after immersing in PBS.

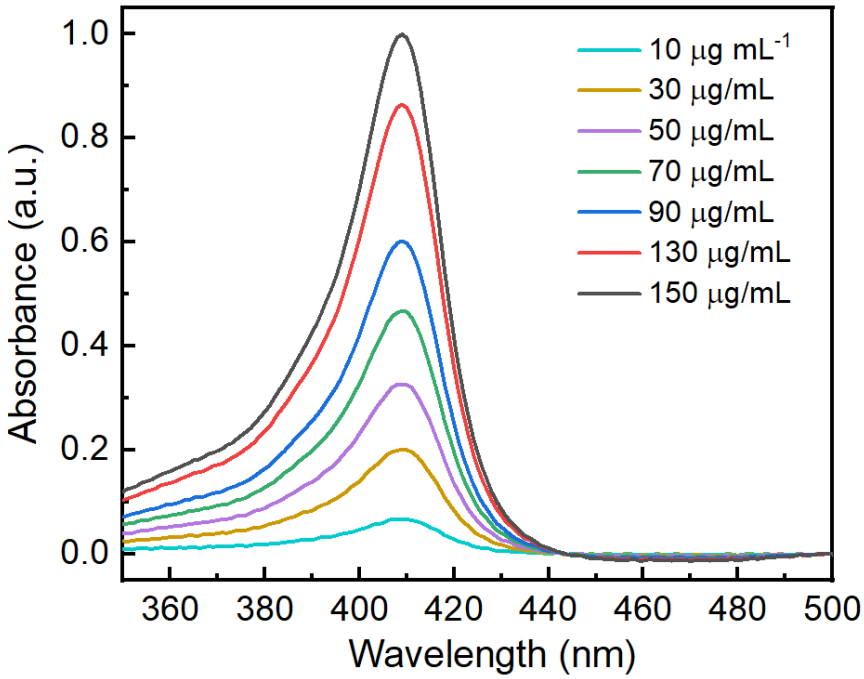

Figure S39. UV-vis spectrum for Mb with different concentrations, which is the data for a standard curve.

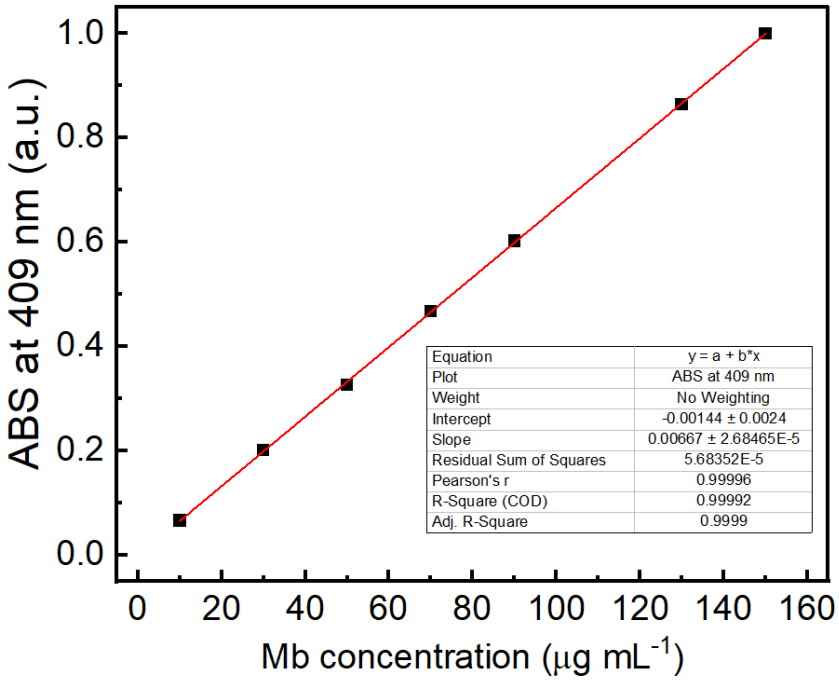

Figure S40. The standard curve of Mb concentrations.

Section S11. 3D COFs with mesopores

Table S5. 3D COFs containing mesopores (large than 2 nm) reported so far.

Material	Linkage	Topology	S_{BET} (m^2/g)	Pore size (nm)	Application	Ref.
DBA-3D-COF 1	Boronate ester	**bor**	5083	2.8	C_2H_6/C_2H_4 separation	[S35]
Ni-DBA-3D-COF			4763	2.6		
SPB-COF-DBA	Boronate ester	**nbo**	1726	2.45	/	[S36]
RICE-3	imine	**pto**	720	1.0, 1.4, 3.2, 4.6	CO_2 uptake	[S37]
RICE-4			654	4.5		
RICE-5			649	4.6		
RICE-6			1612	4.4		
JUC-589	imine	**bcu**	2482	2.1, 2.3	CO_2 separations	[S38]
JUC-551	imine	**dia**	1728	1.4, 2.2	/	[S27]
JUC-552			3023	2.6		
JLNU-320	imine	**dia**	3470	3.3	Rh6G adsorption	[S26]
JUC-564	imine	**stp**	3300	4.3	Mb adsorption	[S39]
Trip-COF 1	imine	**stp**	1473	1.3, 3.0, 4.0	/	[S40]
Trip-COF 2			1624	1.3, 3.0		
HFPTP-TAE	imine	**stp**	1970	4.1	Lipase inclusion	[S41]
HFPTP-DMeTAB			2870	4		
TUS-64	imine	**stp**	1632	4.7	Drug loading	[S42]
3D-bor-COF-1	imine	**bor**	3205	3.1	Benzene vapor adsorption	[S43]
3D-bor-COF-2			1752	3.6		
3D-bor-COF-3			2077	3.8		
3D pts COF	imine	**pts**	3478	2.1	CO_2 separations	[S44]
JUC-561	imine	**ffc**	2359	2.46	Iodine capture	[S45]
COF-790	imine	**fjh**	2650	2	/	[S46]
COF-791			1920	2.3		
COF-792			2250	2.2		

JUC-596	imine	**hea**	2629	1.62, 2.64	H_2 adsorption	[S47]
JUC-597			1857	1.58, 2.59		
3D-lnj-COF	imine	**lnj**	1160	2.65	Gas adsorption	[S48]
NJU-318	imine	**she**	2916	1.5, 3.0	CO_2 Photoreduction	[S49]
NJU-319			1511	1.5, 3.0		
3D-scu-COF-1	imine	**scu**	2340	1.2, 1.6, 1.9, 2.9	Lithium−sulfur batteries	[S50]
3D-scu-COF-2			1602	1.1, 1.7, 2.1, 3.0		
JUC-621	imine	**qtz**	2060	2.3	Iodine capture	[S32]
M-COF	imine	**zyg**	1226	3.4	photocatalysis	[S51]
N-COF			1696	3.4		
S-COF			1383	3.5		
T-COF			891	3.4		
JUC-301	imine	**dia**	607	2.0, 3.7	Mb adsorption	This work
JUC-302			250	5.2		

Section S12. Reference

[S1] Uribe-Romo F. J., Hunt J. R., Furukawa H., Klock C., O'Keeffe M., Yaghi O. M., *J. Am. Chem. Soc.* **2009**, *131*, 4570-4571.

[S2] Wang M., Zeng T., Yu Y., Wang X., Zhao Y., Xi H., Zhang Y.-B., *J. Am. Chem. Soc.* **2024**, *146*, 1035-1041.

[S3] Yu X., Li C., Chang J., Wang Y., Xia W., Suo J., Guan X., Valtchev V., Yan Y., Qiu S., Fang Q., *Angew. Chem. Int. Ed.* **2022**, *61*, e202200820.

[S4] Fang Q. R., Wang J. H., Gu S., Kaspar R. B., Zhuang Z. B., Zheng J., Guo H. X., Qiu S. L., Yan Y. S., *J. Am. Chem. Soc.* **2015**, *137*, 8352-8355.

[S5] Xu X. Y., Cui Q. R., Chen H. Z., Huang N., *J. Am. Chem. Soc.* **2023**, *145*, 24202.

[S6] Wang X. H., Wada Y., Shimada T., Kosaka A., Adachi K., Hashizume D., Yazawa K., Uekusa H., Shoji Y., Fukushima T., Kawano M., Murakami Y., *J. Am. Chem. Soc.* **2024**, *146*, 1832-1838.

[S7] Zhang Y.-B., Su J., Furukawa H., Yun Y., Gándara F., Duong A., Zou X., Yaghi O. M., *J. Am. Chem. Soc.* **2013**, *135*, 16336-16339.

[S8] Ma Y. X., Li Z. J., Wei L., Ding S. Y., Zhang Y. B., Wang W., *J. Am. Chem. Soc.* **2017**, *139*, 4995-4998.

[S9] Cui W.-R., Chen Y.-R., Xu W., Liu K., Qiu W.-B., Li Y., Qiu J.-D., *Sep. Purif. Technol.* **2023**, *306*, 122726.

[S10] Zou J., Wen D., Zhao Y., *Dalton Trans* **2023**, *52*, 731-736.

[S11] Hou B., Yang S., Yang K., Han X., Tang X., Liu Y., Jiang J., Cui Y., *Angew. Chem. Int. Ed.* **2021**, *60*, 6086-6093.

[S12] Zhang M. H., Fang J., Liu Y. Z., Wang Y. J., Liao L., Tang L. X., Zhu L. K., Qiu S. L., Fang Q. R., *Small Structures* **2021**, *2*, 2000108.

[S13] Ma T. Q., Kapustin E. A., Yin S. X., Liang L., Zhou Z. Y., Niu J., Li L. H., Wang Y. Y., Su J., Li J., Wang X. G., Wang W. D., Wang W., Sun J. L., Yaghi O. M., *Science* **2018**, *361*, 48-52.

[S14] Fang J., Fu Z., Chen X., Liu Y., Chen F., Wang Y., Li H., Yusran Y., Wang K., Valtchev V., Qiu S., Zou B., Fang Q., *Angew. Chem. Int. Ed.* **2023**, *62*, e202304234.

[S15] Zhang Y., Li H., Chang J., Guan X., Tang L., Fang Q., Valtchev V., Yan Y., Qiu S., *Small* **2021**, *17*, 2006112.

[S16] Chen F., Guan X., Li H., Ding J., Zhu L., Tang B., Valtchev V., Yan Y., Qiu S., Fang Q., *Angew. Chem. Int. Ed.* **2021**, *60*, 22230-22235.

[S17] Han X., Huang J., Yuan C., Liu Y., Cui Y., *J. Am. Chem. Soc.* **2018**, *140*, 892-895.

[S18] Han J., Feng J., Kang J., Chen J. M., Du X. Y., Ding S. Y., Liang L., Wang W., *Science* **2024**, *383*, 1014-1019.

[S19] Guan P., Qiu J., Zhao Y., Wang H., Li Z., Shi Y., Wang J., *Chem. Commun.* **2019**, *55*, 12459-12462.

[S20] Zhang C.-R., Qi J.-X., Cui W.-R., Chen X.-J., Liu X., Yi S.-M., Niu C.-P., Liang R.-P., Qiu J.-D., *Sci. China Chem.* **2023**, *66*, 562-569.

[S21] Zhang C.-R., Cui W.-R., Yi S.-M., Niu C.-P., Liang R.-P., Qi J.-X., Chen X.-J., Jiang W., Liu X., Luo Q.-X., Qiu J.-D., *Nat. Commun.* **2022**, *13*, 7621.
[S22] Guan X. Y., Ma Y. C., Li H., Yusran Y., Xue M., Fang Q. R., Yan Y. S., Valtchev V., Qiu S. L., *J. Am. Chem. Soc.* **2018**, *140*, 4494-4498.
[S23] Lu Q., Ma Y., Li H., Guan X., Yusran Y., Xue M., Fang Q., Yan Y., Qiu S., Valtchev V., *Angew. Chem. Int. Ed.* **2018**, *57*, 6042-6048.
[S24] Li Z., Li H., Guan X., Tang J., Yusran Y., Li Z., Xue M., Fang Q., Yan Y., Valtchev V., Qiu S., *J. Am. Chem. Soc.* **2017**, *139*, 17771-17774.
[S25] Wang C., Wang Y., Ge R., Song X., Xing X., Jiang Q., Lu H., Hao C., Guo X., Gao Y., Jiang D., *Chem. Eur. J.* **2018**, *24*, 585-589.
[S26] Ma Y., Li J., Sun D., Wu Y., Liu C., Li H., *ACS Appl. Mater. Inter.* **2024**, 10.1021/acsami.4c10591.
[S27] Wang Y. J., Liu Y. Z., Li H., Guan X. Y., Xue M., Yan Y. S., Valtchev V., Qiu S. L., Fang Q. R., *J. Am. Chem. Soc.* **2020**, *142*, 3736-3741.
[S28] Yan D., Lin E., Jin F., Qiao S., Yang Y., Wang Z., Xiong F., Chen Y., Cheng P., Zhang Z., *J. Mater. Chem. A* **2021**, *9*, 27434-27441.
[S29] Wu C., Liu Y., Liu H., Duan C., Pan Q., Zhu J., Hu F., Ma X., Jiu T., Li Z., Zhao Y., *J. Am. Chem. Soc.* **2018**, *140*, 10016-10024.
[S30] Gui B., Xin J., Cheng Y., Zhang Y., Lin G., Chen P., Ma J. X., Zhou X., Sun J., Wang C., *J. Am. Chem. Soc.* **2023**, *145*, 11276-11281.
[S31] Wang K. X., Hou B., Dong J. Q., Niu H. L., Liu Y., Cui Y., *J. Am. Chem. Soc.* **2024**, *146*, 21466-21475.
[S32] Liu Y., Li J., Lv J., Wang Z., Suo J., Ren J., Liu J., Liu D., Wang Y., Valtchev V., Qiu S., Zhang D., Fang Q., *J. Am. Chem. Soc.* **2023**, *145*, 9679-9685.
[S33] Liu M. H., Kong H. Y., Bi S., Ding X. S., Chen G. Z., He J., Xu Q., Han B. H., Zeng G. F., *Adv. Funct. Mater.* **2023**, *33*, 2302637.
[S34] Zhang L., Wang D., Cong M., Jia X., Liu Z., He L., Li C., Zhao Y., *Chem. Commun.* **2023**, *59*, 4911-4914.
[S35] Baldwin L. A., Crowe J. W., Pyles D. A., McGrier P. L., *J. Am. Chem. Soc.* **2016**, *138*, 15134-15137.
[S36] Wang X., Bahri M., Fu Z., Little M. A., Liu L., Niu H., Browning N. D., Chong S. Y., Chen L., Ward J. W., Cooper A. I., *J. Am. Chem. Soc.* **2021**, *143*, 15011-15016.
[S37] Zhu D., Zhu Y., Chen Y., Yan Q., Wu H., Liu C. Y., Wang X., Alemany L. B., Gao G., Senftle T. P., Peng Y., Wu X., Verduzco R., *Nat. Commun.* **2023**, *14*, 2865.
[S38] Liao L., Guan X., Zheng H., Zhang Z., Liu Y., Li H., Zhu L., Qiu S., Yao X., Fang Q., *Chem. Sci.* **2022**, *13*, 9305-9309.
[S39] Li H., Ding J. H., Guan X. Y., Chen F. Q., Li C. Y., Zhu L. K., Xue M., Yuan D. Q., Valtchev V., Yan Y. S., Qiu S. L., Fang Q. R., *J. Am. Chem. Soc.* **2020**, *142*, 13334-13338.
[S40] Wang Y. C., Wu C. Y., Sun W. J., Pan Q. Y., Hao W. B., Liu H., Sun J., Li Z. B., Sun J. L., Zhao Y. J., *Mat Chem Front* **2021**, *5*, 944-949.
[S41] Liu H. Y., Zhou Y., Guo J. B., Feng R., Hu G. L., Pang J. D., Chen Y., Terasaki

O., Bu X. H., *J. Am. Chem. Soc.* **2023**, *145*, 23227-23237.
[S42] Zhao Y., Das S., Sekine T., Mabuchi H., Irie T., Sakai J., Wen D., Zhu W., Ben T., Negishi Y., *Angew. Chem. Int. Ed.* **2023**, *62*, e202300172.
[S43] Li Z. L., Hsueh C. H., Tang Z. Z., Chen J., Wang X. L., Cui H., Yang Y., Wang X. D., Ren D. S., Gao H. Q., Li M. Y., Xu H., He X. M., *SusMat* **2022**, *2*, 197-205.
[S44] Chen L., Gong C., Wang X., Dai F., Huang M., Wu X., Lu C. Z., Peng Y., *J. Am. Chem. Soc.* **2021**, *143*, 10243-10249.
[S45] Chang J. H., Li H., Zhao J., Guan X. Y., Li C. M., Yu G. T., Valtchev V., Yan Y. S., Qiu S. L., Fang Q. R., *Chem. Sci.* **2021**, *12*, 8452-8457.
[S46] Nguyen H. L., Gropp C., Ma Y., Zhu C., Yaghi O. M., *J. Am. Chem. Soc.* **2020**, *142*, 20335-20339.
[S47] Yu C., Li H., Wang Y., Suo J., Guan X., Wang R., Valtchev V., Yan Y., Qiu S., Fang Q., *Angew. Chem. Int. Ed.* **2022**, *61*, e202117101.
[S48] Li Z. L., Xu G. J., Zhang C. X., Ma S., Jiang Y. X., Xiong H., Tian G., Wu Y. Z., Wei Y., Chen X., Yang Y., Wei F., *J. Am. Chem. Soc.* **2024**, *146*, 4327-4332.
[S49] Dong P., Xu X., Luo R., Yuan S., Zhou J., Lei J., *J. Am. Chem. Soc.* **2023**, *145*, 15473-15481.
[S50] Liu W., Gong L., Liu Z., Jin Y., Pan H., Yang X., Yu B., Li N., Qi D., Wang K., Wang H., Jiang J., *J. Am. Chem. Soc.* **2022**, *144*, 17209-17218.
[S51] Ma T. T., Huang G. Z., Wang X. H., Liang Y., Li R. H., Wang B., Yao S. J., Liao J. P., Li S. L., Yan Y., Lan Y. Q., *Natl. Sci. Rev.* **2024**, *11*, nwae177.